Processing at Primary Chemosensory Neurons

Thesis by

Dhruv Zocchi

In Partial Fulfillment of the Requirements for the degree of

Doctor of Philosophy

CALIFORNIA INSTITUTE OF TECHNOLOGY

Pasadena, California

2020

(Defended January 28. 2020)

ACKNOWLEDGEMENTS

Giovanni Zocchi, Mukta Zocchi, Angelica Zocchi
Elena Zocchi, Lina Zocchi, Mahendra Pal Singh, Uma Singh
Rae Demars

I would like to thank my advisors, Yuki Oka and Elizabeth Hong, who saw me start, and end, graduate school, respectively.

I also want to thank the members of my thesis committee, Michael Dickinson, Markus Meister, and Paul Sternberg for their help and support throughout.

ABSTRACT

Chemosensory perception involves the detection of chemical compounds. In animals, there are 2 chemical senses: taste, and olfaction. The two are related in that they utilize ligand-gated receptors, expressed in primary sensory neurons, to detect chemical stimuli from the surrounding environment. However, the processing of these inputs is quite different in the two systems, leading to divergent roles for olfaction and taste in sensory perception. This dissertation highlights some of these differences, by looking at processing of ethologically relevant stimuli at the very peripheral receptor neurons. The work is divided into 2 parts: water sensing by the mammalian taste system, and CO_2 sensing by the *Drosophila* olfactory system.

In Chapter 1, I talk about water sensing in the mammalian taste system. Initiation of drinking behavior relies on peripheral water detection. It is likely that this detection is mediated, at least in part, by the taste system. Here, I have shown that acid-sensing taste receptor cells (TRCs) that were previously suggested as the sensors for sour taste, also respond to water. This response is mediated by a bicarbonate-dependent molecular mechanism, likely involving the Carbonic Anhydrase enzyme family. Furthermore, optogenetic stimulation of the acid-sensing TRCs in thirsty animals induces robust licking responses towards the light source, even in the absence of water. Conversely, thirsty animals lacking functional acid-sensing TRCs show compromised discrimination between water and non-aqueous fluids. Taken together, this work reveals the c*ellular mechanism of water detection by the mammalian taste system*.

In chapter 2, I talk about CO_2 sensing in the fruit fly. The *Drosophila* olfactory system responds to most odors with the activation of a large subset of its olfactory receptors (ORs). This broad activation is a consequence of the ORs having affinity to multiple chemical compounds. In contrast, a small number of odors, like CO_2, elicit responses in only single ORs. These ORs are, in contrast to most ORs, very narrowly tuned, generally responding only to that one odor. It has been assumed up until now that the specificity of these unique ORs is inherited by the olfactory receptor neurons (ORNs) they are

expressed in, and even in the projection neurons (PNs), that the ORNs synapse onto. I show here that CO_2, though it activates only a single OR, the GR63a/GR21a hetero-dimer complex, actually activates multiple ORN axon terminals. This activation is due to lateral excitatory connections between axon terminals of the GR63a/GR21a expressing ORNs, and at least 4 other ORN types. Focusing on one of these ORNs, Ab1B, I show the lateral connections bypass the ORN cell bodies, only driving responses at the axon terminals. Consequently, Ab1B ORN axon terminals receive 2 sources of excitatory input, a feed-forward excitation from its endogenous OR, and a lateral excitation from GR63a/GR21a. This effectively divides the ORN into 2 compartments, distinct in their odor tuning. Finally, I show that lateral excitation is a general feature of the ORN circuit by silencing the feed-forward input of another ORN class, Ab1A. The Ab1A cell body is completely silent, but the axon terminals retain odor responses from lateral excitatory inputs. Thus, there is a *lateral flow of odor information between multiple ORNs of the Drosophila olfactory system*.

PUBLISHED CONTENT AND CONTRIBUTIONS

Zocchi, D., Wennemuth, G., Oka, Y. (2017). "The Cellular Mechanism for Water Detection in the Mammalian Taste System." In: *Nature Neuroscience* 20, pp. 927-933. doi: 10.1038/nn.4575

DZ participated in the conception of the project, carried out the experiments, analyzed data, and wrote the manuscript.

TABLE OF CONTENTS

Acknowledgements....iv
Abstract....v
Published Content and Contributions....vii
Table of Contents....viii
List of Illustrations and/or Tables....ix
Author note....x

Chapter I: The detection of water by the mammalian taste system....1
Introduction....2
Water elicits responses from the taste system....2
Acid sensing TRCs are responsible for water responses....4
Carbonic anhydrases function as molecular detectors for water....5
Optogenetic activation of sour sensing TRCs drives appetitive licking responses in thirsty mice....6
Silencing acid sensing TRCs affects fluid discriminatory ability in thirsty mice....8
Silencing acid sensing TRCs does not affect aversion to sour tastants....9
Discussion....9
Methods....11
References....42
Chapter II: Lateral flow of information at primary olfactory afferents....46
Introduction....47
Multiple ORN classes respond to CO_2....48
VA2 CO_2 responses switch from a low to high responsive state....49
Mismatch in odor tuning between VA2 ORN soma and axon terminals....50
CO_2 responses in VA2 originate from activity in V…....51
DM1 ORNS also receive lateral inputs…....53
Mixed excitation and inhibition confers special response Properties on ORN axons…....54
Discussion…....55
Methods…....58
References…....81

LIST OF FIGURES

Chapter 1 *Page*

1. Water responses in the mammalian taste system 16
2. Water activates the acid sensing taste pathway 18
3. Carbonic anhydrases mediate taste responses to water 20
4. Stimulation of acid sensing TRCs drives drinking responses 22
5. Genetic ablation of ChR2-positive geniculate neurons by DTx 24
6. Water induced taste signals provide a cue for fluid discrimination 26
7. Acid sensing taste pathway is not essential for sour aversion 28
8. Ionic effects on taste responses induces by water 30
9. Taste responses in TRPM5 KO and PKD2L1^{TeNT} mice 32
10. CA independent taste responses and the kinetics of PKD-2L1 taste responses 34
11. Light-induced taste nerve responses in PKD2L1^{ChR2} mice..... 36
12. Ectopic expression of ChR2-EYFP in the geniculate ganglion..... 38
13. Acid-sensing TRCs are important for fluid discrimination, but not for water consumption……..... 40

Chapter 2 *Page*

1. CO_2 elicits responses in multiple glomeruli of the antennal lobe 63
2. CO_2 responses switch from a low to a high state over the course of a recording 65
3. Mismatch in odor tuning between Ab1B cell bodies and axon terminals 67
4. The inhibitory component of the CO_2 response is orco dependent, the excitatory component is Gr21a/Gr21a dependent 69
5. Mismatch in odor tuning between cell bodies and axon terminals of a different olfactory channel..... 71
6. Interaction of inhibitory and excitatory components of CO_2 responses leads to selective filtering of CO_2 versus other odor stimuli……..... 73
7. CO_2 does not drive spiking responses at Ab1B cell bodies……..... 75

8. Odor responses persist in Ab1A terminals when Ab1A cell bodies are silenced…….....77
9. Residual odor responses in Ab1A axon terminals when the Ab1A receptor is silenced are correctly identified as DM1 responses, and not due to out of plane fluorescence…….....79

AUTHOR'S NOTE

The work written about in the first chapter of this thesis was done in the lab of Yuki Oka from October 2014 – March 2017. The work referenced in the second chapter was done in the lab of Elizabeth Hong from January 2017 – July 2019.

Chapter 1

THE DETECTION OF WATER BY THE MAMMALIAN TASTE SYSTEM

SUMMARY

Feelings of thirst trigger water drinking behaviour, which, in turn, is essential for maintaining body fluid homeostasis.[1-3] Initiation of drinking behaviour therefore relies on both internal state, as well as peripheral water detection.[4-7] While the neural circuits underlying thirst have been well studied, it is still unclear how mammals recognize water in the oral cavity. Here, we identified the cellular logic of water taste in the mammalian taste system. We show that a single class of taste receptor cell (TRC) mediates taste responses to water. We identified this cell population as the acid-sensitive taste receptor cells (TRC) that was previously suggested as the sour taste sensor.[8-11] Genetic silencing of these TRCs abolishes water-evoked responses. Conversely, optogenetic stimulation of acid-sensitive TRCs in thirsty animals induced appetitive drinking responses toward light even in the absence of water. Moreover, our functional manipulation studies indicate that the activities of acid-sensitive TRCs are neither necessary nor sufficient to induce aversion, a typical behaviour when animals encounter sour substances. Taken together, these results show that mammalian acid-sensitive TRCs may be used to detect water in the oral cavity.

INTRODUCTION

Oral sensation, which includes the sense of taste, serves as a checkpoint prior to ingestion of nutrients. The mammalian taste system detects and differentiates between essential nutrients as well as toxic substances through taste receptors and channels expressed in TRCs.[8-11,39] As an example, low concentrations of sodium are sensed by a single class of TRCs expressing the epithelial sodium channel, ENaC. Consequently, knocking out the ENaCα gene abolishes appetitive salt intake in mice who have been salt deprived.[12,13] Similarly, there exist dedicated receptors and TRCs for the tastes of L-amino acids, sugars, bitter, and acidic substances.[14-18] Precise genetic access to the 5 different TRC classes is possible via the use of specific protein markers. In particular, acid-sensing TRCs express a protein called polycystic-kidney-disease-like channel[19] (PKD2L1). In contrast to the 5 basic tastes, it is still controversial whether water, another vital body nutrient, is also detected by the taste system in mammals.

Several decades of study have shown that invertebrates such as *Drosophila melanogaster* can sense water through specialized sensory cells in the taste system.[20-22] Recent studies have demonstrated that PPK28, a member of the DEG/ENaC family is required for sensory responses to external water, as well as water-seeking behavior.[22] In vertebrate species such as frogs, sheep, and cats, water has been shown to elicit electrophysiological responses in facial nerves innervating the oral cavity.[23-26] Moreover, water-induced responses have been reported in taste-related neurons of the nucleus of the solitary tract in rodents.[26] While these studies suggested that water perception is partially encoded by the taste system, the underlying sensing mechanisms in mammals have not been elucidated to date.

WATER ELICITS RESPONSES FROM THE TASTE SYSTEM

We reasoned that if the taste system is used to detect water in mammals, at least two criteria should be met; first, water taste should be mediated by specific cellular and molecular substrates in taste buds, and second, activation of this pathway should evoke water taste

sensation to animals. To test the first of these hypotheses, we performed *in vivo* extracellular recordings from the chorda tympani taste nerves to explore water responses. The chorda tympani innervates all 5 TRC classes of the tongue, and so serves as a good conduit to monitor the overall activity of the taste system. Stimulating the tongue with various solutions, we observed robust spiking in response to all 5 basic tastes (Figure 1a), showing that we were effectively able to resolve spiking from each TRC population.

We then tested for water responses by probing the tongue with deionized water, eliciting robust nerve responses (Figure 1a). This demonstrated that water effectively activates the taste system, presumably driving responses in 1 or more TRC classes. How does application of deionized-water induce spiking in TRCs? The mammalian oral cavity is normally covered with a thin layer of saliva containing various ions and enzymes.[27,28] Our experiments were done in deeply anesthetized animals. A consequence of the anesthetization is that the mice stop producing any saliva. Therefore, we had to constantly perfuse into the oral cavity an artificial saliva solution made up of the ionic components of normal saliva. Tastant and water stimuli were then presented sandwiched between artificial saliva perfusion.

The water responses we measured were therefore due to the wash out of the ions present in saliva with pure deionized water. These observations indicate that the ionic constituents of saliva play a key role in gating the responses. Is any one of these ions particularly important? We sought to answer this question by making salt solutions of each of the ions present in artificial saliva, and assessing whether we could induce water responses by switching from perfusion of the single salt solution to perfusion of deionized water. Intriguingly, we found that the responses to water were only triggered when bicarbonate ion solutions were used. In other words, changing from bicarbonate solution to water triggered robust nerve responses (Figure 1b, upper middle panel), whereas bicarbonate-free saliva followed by water application failed to induce responses (Figure 1b, upper right panel). No other ions in artificial saliva induced significant taste responses (Figure 1b, lower panel), although high concentrations of phosphate exhibited minor responses (Extended Data Figure 1a). Indeed, potassium bicarbonate in baseline solution evoked dose-dependent nerve responses when

switched to water while potassium chloride had no effect (Figure 1c). Together, these results point out two important characteristics of taste responses to water; 1) the responses are induced by washing out of saliva with water, and 2) unlike invertebrate water detection,[22] osmolality change by itself is not the key determinant.

When animals are thirsty, they selectively drink water over other fluids (i.e. oils). If the observed responses are the basis of water detection, one would expect the responses to be selective for aqueous solutions. In fact, application of non-aqueous silicone oil on the tongue did not evoke any significant nerve responses compared to water, indicating that the responses require aqueous solution on the oral cavity (Figure 1d).

ACID SENSING TRCS ARE RESPONSIBLE FOR WATER RESPONSES

Our results above indicate that one of the 5 TRC classes is driving responses to water. We therefore sought to identify the cellular substrate mediating these water taste responses. Previous studies have identified genetic markers that specifically label TRCs encoding individual taste qualities.[8,14-19,29] Using these genetic handles, we systematically silenced the different TRC classes to assess which class is required for water responses. Transgenic animals lacking TRPM5, a key transduction channel for umami, sweet, and bitter,[29] are unable to detect these three taste modalities, due to silencing of the corresponding TRC classes (Figure 2a). In these animals, nerve responses to water were unaffected and indistinguishable from those in control animals (Figure 2a and Extended Data Figure 2a). This shows that the water responses are completely independent of the activity of the sweet, umami, and bitter sensing TRCs. Similarly, inhibiting the function of the sodium taste sensor, ENaC, by application of its antagonist (amiloride[30]) entirely suppressed sodium-evoked responses, but had no significant effect on nerve responses to water (Figure 2b). Therefore, the salt sensing TRCs can also be ruled out as the source of the water responses. Finally, we examined the involvement of acid-sensitive TRCs by genetically silencing their synaptic

machinery. To achieve this, we used transgenic animals where the tetanus toxin subunit was targeted to PKD2L1-positive cells by crossing Cre-dependent toxin (TeNT) and PKD2L1-Cre transgenic mouse lines[31] (PKD2L1^{TeNT}). Surprisingly, disrupting synaptic transmission from acid-sensitive TRCs resulted in a total loss of water responses (Figure 2c) without affecting other taste qualities, with the exception of acid responses (Extended Data Figure 2b). Altogether, these results show that the acid-sensitive taste pathway is the cellular substrate for chorda tympani responses to water.

CARBONIC ANHYDRASES FUNCTION AS MOLECULAR DETECTORS FOR WATER

How does water drive acid-sensing TRCs to spike? Given a function of PKD2L1-expressing TRCs as acid sensors (Figure 2c), one possibility is that the water stimulus is converted to a local pH change, leading to the activation of this population. Moreover, saliva is buffered by bicarbonate, as well as phosphates, which keep the salivary pH relatively neutral.[42] Given the role of bicarbonate in generating water responses, a pH change mechanism whereby the neutral saliva is replaced by a proton source seemed plausible. Consistent with this notion, water responses were sensitive to saliva pH (Figure 2d). In particular, excessive protons in saliva suppressed water responses, indicating the water responses required the saliva to be relatively pH neutral.

Carbonic anhydrase 4 (CA4) is a membrane-bound catalytic enzyme expressed by acid-sensitive TRCs,[31] which reversibly catalyzes the conversion of bicarbonate and protons into CO_2 and water. We hypothesized that washing out of bicarbonate from saliva reverses this reaction, which in turn increases local proton production. If this is true, pharmacological blocking or knocking out of CA4 should affect water taste responses. In fact, mice lacking CA4 exhibited significant and selective reduction in their water responses although minor residual responses remained (Figure 2e and Extended Data Figure 3a). Similarly, CA blockers like dorzolamide and benzolamide drastically suppressed water responses without

affecting other taste responses (Figure 2f and Extended Data Figure3b). These results suggest that CA4, and perhaps other CAs, function as molecular detectors that translate water stimuli into a local pH drop (Extended Data Figure 3c).

OPTOGENETIC ACTIVATION OF SOUR SENSING TRCS DRIVES APPETTITIVE LICKING RESPONSES IN THIRSTY MICE

Our electrophysiological results addressed the first of the 2 criteria we framed above about water taste responses. We have established that water drives responses in a specific TRC population, and does so via the action of a dedicated molecular mechanism. The second criteria we imposed was that the activity of the dedicated TRC population should signal the presence of water to a thirsty animal. To assess this hypothesis, we utilized an optogenetic strategy by engineering animals expressing the blue light activated ion channel, channelrhodopsin[32] (ChR2) in PKD2L1-expressing TRCs (PKD2L1^{ChR2}, Figure 3a). By illuminating the tongues of these animals with blue light, we could thus effectively drive a large subset of the acid-sensing TRCs. We tested the behavioral consequences of acid-sensing TRC activation by placing the mice in a custom built gustometer with access to a water bottle. The bottle was empty except for a fiber optic cable coupled to a blue laser. The gustometer was set up such that the laser delivered a quick burst of blue light every time the animal licked at the bottle. With this closed loop stimulation setup, we were able to assess the behavioral effects of activating acid-sensing TRCs.

To our surprise, we found that thirsty PKD2L1^{ChR2} mice exhibited vigorous licking responses toward light in the absence of actual water (Figures 3b and c). This behavior was light-intensity dependent (Extended Data Figure 4b), and was observed both in 5-sec brief access tests, where the animals were only allowed access to the bottle for 5 second intervals (Figure 3c), as well as 1-min continuous access tests (Figure 3d, Supplementary Video 1, and 2). In contrast, neither control animals lacking ChR2 expression, or PKD2L1^{ChR2} mice without

photostimulation showed this behavior (Figure 3d). Therefore, artificial stimulation of acid-sensing TRCs can drive appetitive behavior in thirsty mice. If activation of acid-sensitive TRCs indeed provides a cue for water detection, then animals should be attracted to light only when they are thirsty and searching for water. Thus, we explored the effect of photostimulation on various appetites such as sugar consumption in hungry animals (Figure 3f) and salt appetite in sodium-depleted animals (Figure 3g). As predicted, animals exhibited no behavioral attraction toward light under hungry and salt-craving conditions (Figures 3f and g). Together, these results satisfy the second criteria we imposed for water responses.

We next asked whether long term activation of acid-sensitive TRCs may lead to satiation of thirst. Thirsty animals normally drink to satiety within few minutes when water is available (Figure 3e, black). Remarkably, water-deprived PKD2L1^{ChR2} animals showed continuous and unimpeded licking toward light during longer term behavioral sessions lasting 10 min (Figure 3e, red). However, in the presence of water, animals stopped drinking after satiation even with photostimulation (Figure 3e, gray). Together, these results clearly demonstrate that activation of acid-sensitive TRCs serves as a cue for the presence of water, but does not by itself serve as a satiation signal.

In addition to the expression in taste buds, we noticed that ChR2 was ectopically expressed in a small number of geniculate neurons, secondary taste neurons that innervate taste buds (Extended Data Figure 5). To eliminate the possibility that these neurons are involved in light-dependent drinking responses, we expressed Cre-dependent diphtheria toxin receptor in the background of PKD2L1^{ChR2} (PKD2L1^{ChR2}/DTR) and ablated PKD2L1-expressing cells by injection of diphtheria toxin. Since TRCs, but not secondary neurons, regenerate over time, we were thus able to eliminate the contribution of ChR2-positive geniculate neurons. After regeneration of TRCs, we confirmed that PKD2L1^{ChR2}/DTR mice still show drinking response toward light demonstrating that the behavior is driven by the activity of TRCs (Figure 4).

SILENCING ACID SENSING TRCS AFFECTS FLUID DISCRIMINATORY ABILITY IN THIRSTY MICE

External water is likely detected through multiple orosensory systems including taste and tactile signals.[33] To what extent is signaling through the acid-sensing TRCs used for identifying water? In the complete absence of taste responses to water (e.g. PKD2L1^{TeNT} mice), animals show normal spontaneous as well as thirst-induced drinking (Extended Data Figures 6a and b). These data suggest that the taste pathway is not required for proper water identification and consumption. Instead, we wondered whether the taste pathway may play a role in discriminating water from other non-aqueous liquids. To test this idea, PKD2L1^{TeNT} and control animals were water-deprived, and then given a choice between water and low-viscosity silicon oil in a brief taste preference test. Not surprisingly, the control group showed a strong preference to water over silicone oil (Figures 4a and c, and Extended Data Figures 6c and d). However, in sharp contrast, PKD2L1^{TeNT} animals failed to discriminate these two fluids, consuming both silicon oil and water (Figures 4b and c). In fact, PKD2L1^{TeNT} animals consumed significantly more silicone oil and less water compared to the control group. We observed a similar effect when using mineral oil, another taste-less fluid (Extended Data Figure 6e), although the animals eventually learned to avoid the non-aqueous stimulus, no doubt using non-taste sensory cues. Note that PKD2L1^{TeNT} mice showed normal attraction to sweet and aversion to bitter compounds (Figure 4d), indicating that they retain taste discrimination ability. Thus, signals via the acid-sensitive taste pathway provide a cue for fluid choice and subsequent water intake.

SILENCING ACID SENSING TRCS DOES NOT AFFECT AVERSION TO SOUR TASTANTS

Previous studies have shown that acids activate PKD2L1-expressing TRCs, and eliminating these cells abolishes acid-evoked taste nerve responses.[10,11,19] Based on these findings, the PKD2L1-expressing TRC population has been suggested to mediate both sour taste and

behavioral aversion. However, our results show that these TRCs can mediate both electrophysiological responses as well as behavioral attraction to water. To address this apparent conflict, we investigated if PKD2L1-expressing TRCs are required for behavioral aversion to sour tastants. Control animals with intact acid taste sensors exhibit robust aversion to citric acid (Figure 5a, left panel). In contrast, we observed similar levels of aversion in PKD2L1^{TeNT} animals where the taste nerve responses to the acid were eliminated (Figure 5a, right panel). These data show that the taste pathway is not required for behavioral aversion to acids. On the other hand, optogenetic stimulation of the same population with ChR2 (PKD2L1^{ChR2} animals) triggered dose-dependent robust taste nerve firing (Figure 5b, left panel). These mice, however, showed no aversion toward water in the presence of light at any intensity (Figure 5b, right panel). Although PKD2L1-expressing TRCs are acid sensitive, our loss-of-function and gain-of-function experiments indicate that this population may not be directly involved in behavioral aversion associated with sour taste.

DISCUSSION

Peripheral water detection represents the first step in the process leading to ingestion and subsequent satiation of thirst. Since Zotterman first described water taste responses in frogs several decades ago,[23] accumulating evidence supports the presence of taste detection mechanisms for water in various vertebrate species.[23-26,35] Here, we used *in vivo* electrophysiology to elucidate mechanisms underlying water taste responses. We showed that washing out saliva with water activates the acid-sensitive taste pathway through PKD2L1-expressing TRCs. Furthermore, our data implicate that the removal of bicarbonate in saliva leads to a local pH change through the activity of CAs expressed in PKD2L1-expressing TRCs. Because over 99% of saliva is water, it seems logical that the taste system has a mechanism to detect the dilution of ions, specifically bicarbonate, as a signal of incoming water, rather than sensing water itself. Together, these studies provide key insights into the cellular and molecular basis of water detection at the periphery.

It has been previously demonstrated that PKD2L1-expressing TRCs are activated by acids, salts, and CO_2.[19,31,34,36,37] All 3 of these substances elicit aversive behavioral responses from mice. On the basis of these aversive behaviors, the acid-sensing TRCs were thought to encode an innate aversion, possibly linked to the sour taste perception. We now add water to the list of stimuli that activate acid-sensing TRCs. Given this large breadth of tuning, the question arises of what taste information these TRCs encode. In this study, we show that optogenetic activation of this taste pathway by light triggered appetitive licking responses in thirsty animals. Inactivation of the same population compromised animals' fluid discriminability, demonstrating the importance of this pathway for attraction towards, and proper discrimination of water. Conversely, silencing PKD2L1-expressing TRCs had no effect on acid-induced aversive behavior. These results argue that this taste pathway by itself plays a minor role in aversion towards sour, or any other noxious substances. It may, however, be involved in sour perception/aversion under different circumstances such as in combination with other sensory signals. For example, besides the taste system, other sensory pathways including the trigeminal system also contribute to orosensation.[33] Because various noxious chemicals are known to activate both taste and trigeminal nerves,[36] it is conceivable that behavioral aversion to acids, salt, and CO_2 is mediated by neurons in the trigeminal system in combination with signals from acid-sensing TRCs. Perceptual differences between water and sour tasting compounds may then be accounted for by the combinatorial activation of acid-sensitive TRCs and trigeminal nerves. One possible explanation is that activity in the acid-sensing TRCs alone encodes water perception, while sour perception may be created when both taste and trigeminal pathways are activated.

Notably, behavioral attraction by photostimulation of the water taste pathway was induced only when animals were dehydrated, but not food or salt depleted. Therefore, unlike sweet or bitter tastes that are linked to positive and negative values independent of internal state,[40] the valence from the water taste pathway is internal-state dependent. The mechanisms underlying this valence change are unknown. While hypothalamic and reward circuits are likely involved in this process,[38,41] peripheral mechanisms may also contribute to this valence

change. Future studies with neural manipulations of peripheral water pathway and central thirst circuits should help address how appetite and valence of water are encoded in the brain.

METHODS

Animals

All procedures were carried out in accordance with US National Institutes of Health (NIH) guidelines for the care and use of laboratory animals, and received approval from the Caltech Institutional Animal Care and Use Committees (IACUC). *C57BL/6ByJ* (B6, stock number 000664), *Ai32* (stock number 012569), *Rosa26iDTR* (stock number 008040) mice were obtained from the Jackson Laboratory. Transgenic lines used were *TRPM5 knockout*[29], *PKD2L1-Cre* [8], *Rosa26-flox-TeNT*[41], as described previously. For optogenetic experiments, *PKD*^{Ch2} mice were generated by crossing *PKD2L1-Cre with* Ai32 lines. *Rosa26-flox-DTR* was crossed with *PKD*^{Ch2} line to generate *PKD*^{ChR2}*/DTR* mice for cell-ablation experiments. CA4 knockout mice were provided by Dr. Gunther Wennemuth. Mice used for data collection were both males and females, at least 6 weeks of age. Animals were housed in a temperature-controlled environment with a 13-h light, and 11-h dark cycle, and *ad libitum* access to food and water unless otherwise noted.

Nerve Recordings

Mice were anaesthetized with pentobarbital (100 mg/kg) and placed in a head-fixed setup. Body temperature was monitored and regulated using a closed-loop heating system. Chorda tympani taste nerve recordings were performed as previously described [14,35]. Briefly, animals were given a tracheotomy to prevent suffocation and the right branch of the chorda tympani nerve was exposed. A high impedance tungsten electrode was hooked onto the nerve and a drop of halocarbon oil was dropped inside the surgical cavity. Stimuli were delivered using a pressurized perfusion system (AutoMate Scientific) to keep a constant flow rate. Stimuli used were: 60 mM NaCl (salt), 10 mM Citric Acid (sour), 8 mM acesulfameK (sweet), 0.1 mM cycloheximide (bitter), 50 mM monopotassium glutamate (MPG) plus 1 mM inosine monophosphate (IMP) (umami) and 5 cSt silicone oil (Aldrich), mineral oil (Aldrich).

Deionized water was either filtered (Elaga, PURELAB flex) or purchased (Ultra-purified water, Invitrogen 10977-015). All solutions were used at room temperature. Nerve responses during the 20-s tastant stimulation were integrated and analysed. Responses in each recording session were normalized to 8 mM AceK (Figure 1, 2b, c, e, f, and 5), 10 mM Citric Acid (Figure 2a), and to 25 mM $KHCO_3$ (Figure 1c). For Figure 1b, individual responses were normalized to the average 8 mM AceK responses across entire sessions. The artificial saliva composition was as follows: 4 mM NaCl, 10mM KCl, 6 mM $KHCO_3$, 6mM $NaHCO_3$, 0.5 mM $CaCl_2$, 0.5 mM $MgCl_2$, 0.24 mM K_2HPO_4, 0.24 mM KH_2PO_4. pH was held between 7.4 and 7.6. For Figure 2d, the pH of artificial saliva was adjusted between 6 and 8. To stabilize pH of water in CA4 experiments (Figure 2e), we added 0.2 mM KH_2PO_4 and adjusted pH to 7.5. we Each tastant stimulation was followed by intervals at least for 40 s. Pharmacological experiments were conducted as follows: 50 mM amiloride was dissolved into tastant stimuli solutions and delivered via the pressurized perfusion system. Tastant solutions containing amiloride were presented for 20 s, preceded and followed by 5 s incubation periods with saliva containing the same concentration of amiloride. The oral cavity was incubated with a membrane-impermeable CA blocker, benzolamide (650 μM) or a membrane-permeable blocker, dorzolamide (0.5%) in water for 7 min before washing out with saliva as described previously.[31]

Analysis of activation kinetics of taste nerves

Activation kinetics of nerve responses was analysed in the following manner. The time points of 25% and 75% of maximum amplitude in each response were determined by MATLAB, and the rise time was calculated as the difference between these two points (Extended Data Figure 3d). The ratio of water to sour rising phase slopes was calculated as the slope of the line connecting the points at 25% to 75% of the peak amplitude of the response.

Taste preference assays

Animals were tested in a custom gustometer to measure taste preference as previously described.[14] Solutions were presented to animals for 60 s per trial. Each behavioral session comprised of 10 to 30 trials depending on the number of tastants tested. Each stimulus was presented at least 5 times in one session. Presentations automatically terminated 5 s after the first lick. The number of licks in each of these 5-s windows were counted, and then averaged

across the session. Each animal was tested up to 3 sessions with the same taste repertoire. We freshly prepared solutions for each behavioral experiment to minimize contamination of other sensory cues such as odors. Prior to all behavioural experiments, mice were water restricted for 22-48 h. For experiments that extended for 48 h, animals were provided with 0.5 mL of water after 23 h. For sucrose appetite assays, animals had no access to food for the 23 h prior to the experiments (Figure 3e). For salt appetite assays (Figure 3f), mice were injected with furosemide as previously described[35] and were kept for 23 h with low-sodium diet (Envigo 90228) with free access to water. For sucrose and salt appetite experiments, we used 300 mM sucrose and NaCl. Before testing with photostimulation, animals were pre-trained to drink these solutions.

For drinking assay for silicone oil and water (Extended Figure 6c and d), animals were subjected to water-deprivation for 24 hrs, and either water or silicone oil was presented during the 5-min assay. Individual fluids were tested on separate dates; water tests were normally followed by silicone oil tests because some animals were euthanized after the silicone oil assays due to serious dehydration. We note that both control and PKD2L1^{TeNT} animals preferred water in a long-term ad-lib drinking assay.

For quantifying spontaneous and thirst-driven drinking, animals were individually placed in their home cage and water intake was monitored for 24 hrs (ad-lib), or for 15 min (after water-deprivation for 24 hrs).

Cell ablation by injection of diphtheria toxin

PKD^{ChR2}/DTR mice were given an intra-muscular injection of diphtheria toxin fragment A (20 mg/kg BW per day, Sigma D0564) for 2 consecutive days. Expression of ChR2 on the tongue was monitored before, during, and after injections to assess amount of ablation. After the 2-day injection regime, mice were housed 3-4 weeks before being used for behavioural experiments to allow regeneration of TRCs.

Optogenetic stimulation

Photostimulation of the tongue was performed using a gustometer as described above. Animals were subjected to a brief access taste preference assay as follows; 1) two empty bottles with and without an optic fiber, 2) solutions with and without an optic fiber. Blue laser pulses (430-490 nm, Shanghai Lasers and Optics Century Co.) were delivered through an optic fiber (1mm diameter, ThorLabs) using a pulse generator (World Precision Instruments). The stimulation paradigm was set so that every lick triggered a laser pulse of 1-sec duration in a close-loop manner. The laser power was kept at 48 mW (measured at the tip) unless otherwise noted.

Photostimulation of taste nerves

The same surgery for nerve recording was performed as outlined above. For optogenetic stimulation, the tip of an optic fiber was placed a few millimetres from the tongue while nerve responses from *PKD2L1*^{ChR} were recorded. Trains of light pulses of 20 s duration were flashed onto the tongue. Each 20 s stimulation window was followed by 40 s intervals. Light trains were delivered at 8 Hz, with each pulse of a 40 ms duration. The frequency and duration was determined based on the licking behavior of mice in our behavioural assays, as well as published literature for the B6 strain (4).

Histology

Animals were euthanized with CO_2 followed by cervical dislocation, and perfused with PBS followed by 4% PFA. Tongues were removed and kept in 4% PFA for 12 h followed by 30% sucrose in PBS for overnight. Frozen sections of 20-µm thickness were prepared on slides and were post-fixed with 4% PFA for 15 min. Then the samples were incubated with blocking buffer (10% donkey serum, 0.2% Triton-X) for 2 h before incubation with primary antibodies. Primary antibodies used were goat αCA-4 (R&D Systems, 1:500, AF2414), αGFP (Abcam, 1:1000, ab6673), and rabbit αPLC-β2 (Santa Cruz Biotechnologies, 1:500, sc-206). Rabbit PKD2L1 antibody[9] (1:500) was a generous gift from Dr. Matsunami at Duke University. Secondary antibodies were donkey anti-goat Cy3 (Jackson ImmunoResearch, 1:500, 705-165-147), donkey anti-rabbit Alexa-488 (Jackson ImmunoResearch, 1:500, 711-545-152), andchicken Alexa-488 (Jackson ImmunoResearch, 1:500, 703-545-155).

Acknowledgments

We thank Brittany Ho for help with mouse husbandry. We also thank Drs. Kristin Scott,

Markus Meister, and David J. Anderson for helpful suggestions. We thank Drs. Charles Zuker and Nick Ryba for generously sharing PKD2L1-Cre and TRPM5 KO transgenic animals, Dr. Matsunami for PKD2L1 antibody, Sangjun Lee for technical support, and members of the Oka lab for helpful comments. This work was supported by Startup funds from the President and Provost of California Institute of Technology and the Biology and Biological Engineering Division of California Institute of Technology. Y.O. is also supported by the Searle Scholars Program, the Mallinckrodt Foundation, the Okawa Foundation, McKnight Foundation, and Klingenstein-Simons Foundation. Y.O. have disclosed these methods and findings to the Caltech Office of Technology Transfer.

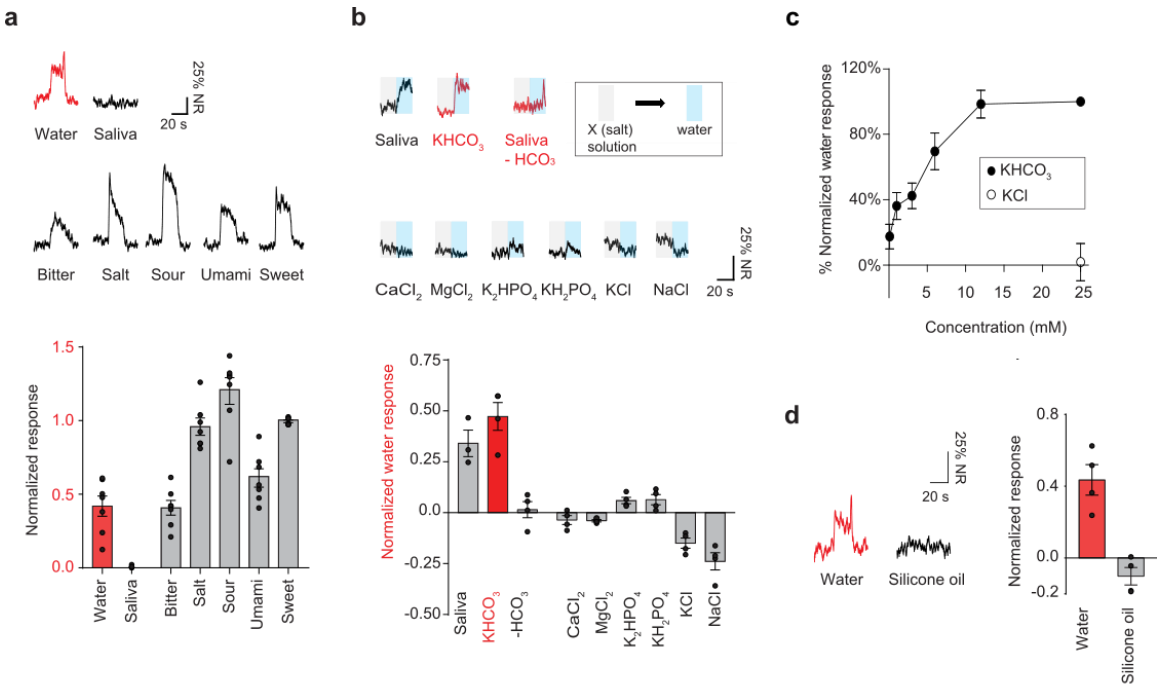

Figure 1

Figure 1: Water responses in the mammalian taste system. a, Water elicits robust responses in chorda tympani taste nerves. Shown are representative integrated chorda tympani nerve responses to water and five basic tastants (upper) and their quantified data (bottom). Application of water evoked significant taste responses (n = 7 mice; p=0.0006, water vs saliva). NR, normalized response. Tastants used were: bitter (0.1 mM cycloheximide), salt (60 mM NaCl), sour (10 mM citric acid), umami (50 mM MPG + 1 mM IMP), sweet (8 mM AceK). Artificially reconstituted saliva solution (see Methods) was used as a base solution for all stimuli. **b**, Effects of individual ion components on water responses. Representative traces are shown (upper) where grey and blue shades denote each salt solution and water, respectively; the trace for saliva minus HCO_3 was from a different animal. Average water responses elicited by different salt solutions were quantified (lower). Removal of bicarbonate ions elicits water responses while saliva lacking bicarbonate ions or other ion species had no effect (n=3 for saliva, n=4 for other solutions; p=0.0286,

$KHCO_3$ vs Saliva - HCO_3). **c,** Dose dependence of water responses to potassium bicarbonate. Higher concentrations of potassium bicarbonate induced larger water responses while potassium chloride elicited no response (n=4). **d,** Washing-out of saliva with non-aqueous silicone oil does not induce response. Shown are representative traces to water and silicone oil (left), and quantification of responses were shown (right, n=4; p=0.0286). Statistical significance was analyzed with two-tailed Mann-Whitney U-test. Values are means ± s.e.m.

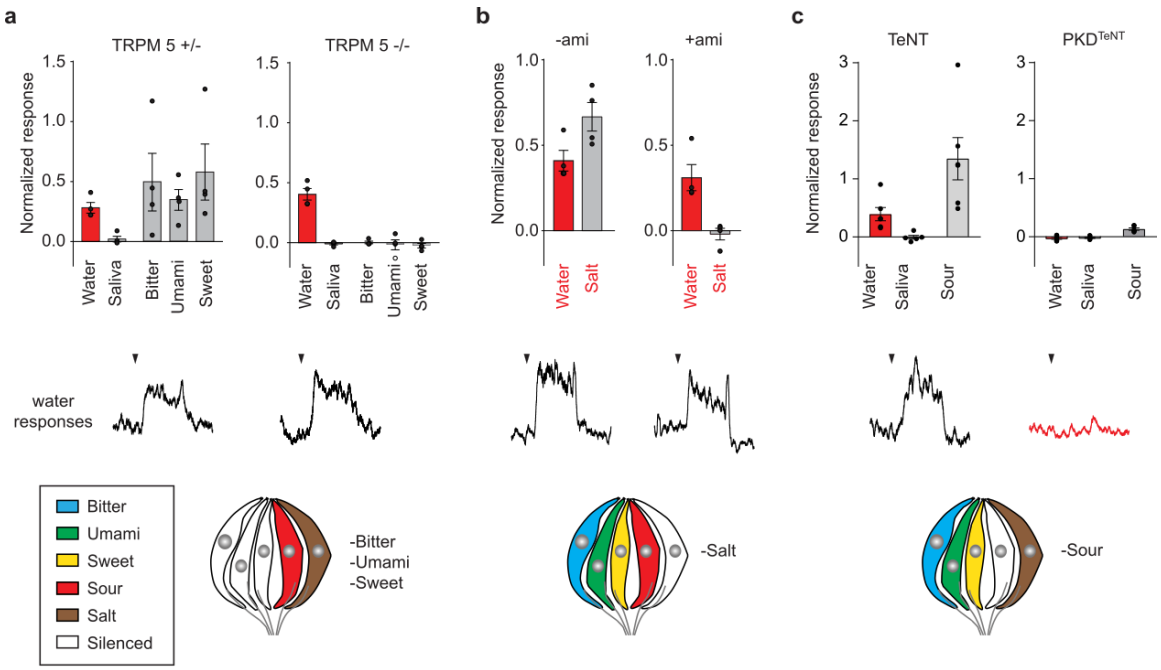

Figure 2

Figure 2: Water activates the acid-sensing taste pathway. a, *Trpm 5 -/-* mice show no responses to bitter, umami, or sweet tastants. However, they retain intact water responses comparable to control animals (n=4 for *Trpm 5 -/-* and *Trpm 5 +/-*). **b**, Application of amiloride (50 μM) completely blocked sodium responses, while it exerted a minor effect on water responses (n=4; p=0.2 for salt). **c**, Silencing acid-sensing TRCs (PKD2L1^{TeNT} mice) eliminated water responses in addition to acid responses, while control animals (TeNT) show normal responses to both (n=5 for saliva in control, n=6 for the rest; p=0.0022 for water). The data demonstrate that the acid-sensing taste pathway is required for taste responses to water.

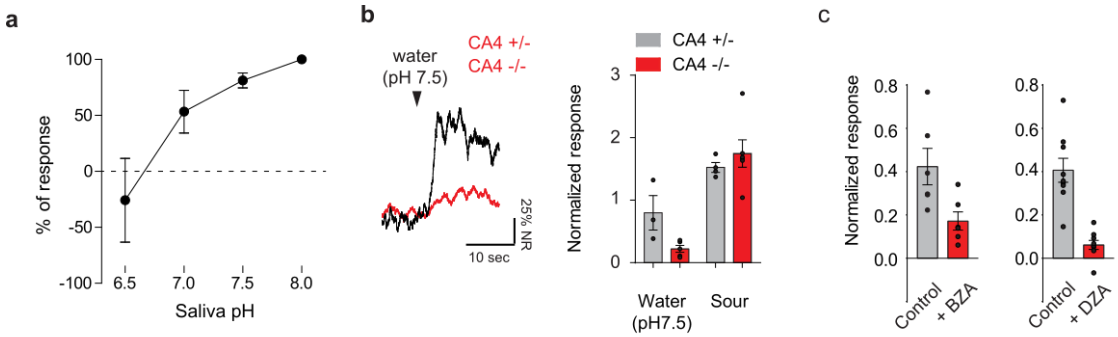

Figure 3

Figure 3: Carbonic anhydrases mediate taste responses to water. a, Water responses are sensitive to saliva pH. All responses are normalized to the responses at pH 8 (n=4; p=0.0392 for pH 6.5 vs pH 7.5, two-tailed paired t-test). Note that saliva pH in healthy animals is normally neutral to basic.[42] **b,** Representative traces from CA4 +/- and -/- mice showing responses to neutral water (adjusted to pH 7.5, left). CA4 -/- have severely reduced responses to water (n=5 for -/-, n=3 for +/-; p=0.0357, two-tailed Mann-Whitney U-test). **c,** Water responses before and after incubation with CA inhibitors, benzolamide (BZA) and dorzolamide (DZA). Both drugs reduced water responses (n=6; p=0.0159 for benzolamide, n=9; p=0.0007 for dorzolamide, two-tailed paired t-test). Values are means ± s.e.m.

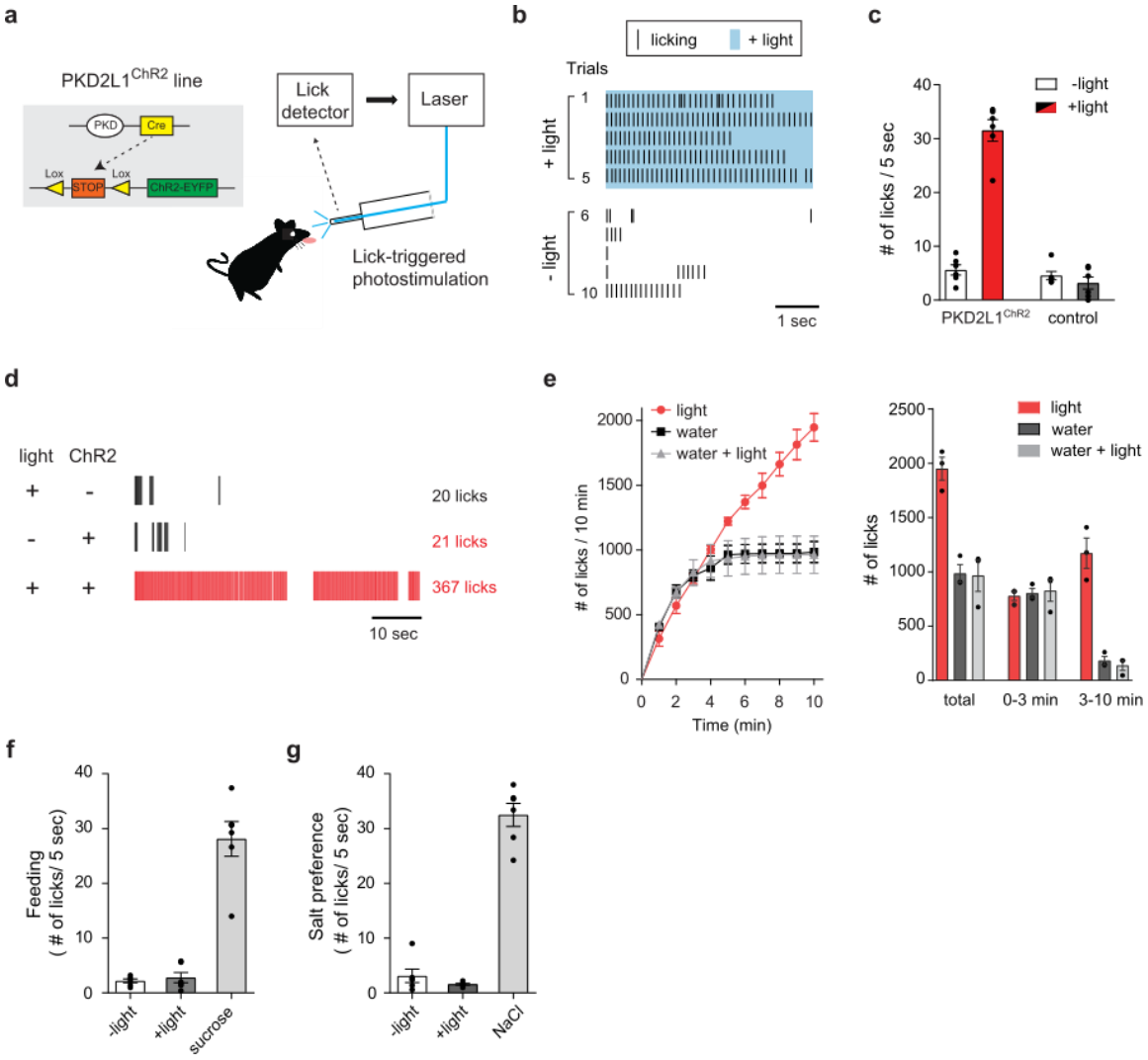

Figure 4

Figure 4: Stimulation of acid-sensing TRCs drives drinking responses. a, A diagram of light-dependent drinking response. Transgenic mice expressing ChR2 in PKD2L1-expressing TRCs (PKD2L1^{ChR2}) were subjected to a close-loop self-stimulation paradigm where each lick event induces 1-sec laser pulse through an optic fiber placed in an empty water spout. **b**, Photostimulation of PKD2L1-expressing TRCs induced robust drinking responses without water (trials 1-5: blue shading). In the absence of light, the same water-deprived animal did not show consistent licking (trials 6-10). Individual black bar indicates

each lick event. **c**, Quantification of light-dependent lick events. Number of licks was counted during the 5-sec window. Each condition was presented more than five trials and the number of licks was averaged across trials. The panel shows PKD2L1^{ChR2} mice (n=6, red bar) and PKD2L1-Cre control mice (n=6, black bar) with photostimulation; white bars indicate the number of licks without light (P=0.0022; two-tailed Mann-Whitney U-test). **d**, Photostimulation induced continuous drinking responses. Shown are representative plots illustrating the drinking responses toward light in a thirsty control animal (top), and PKD2L1^{ChR2} animal without (middle) or with light (bottom) during 1-min session. Total lick numbers are shown (right). **e,** Photostimulation does not satiate animals. Shown are cumulative number of licks from PKD2L1^{ChR2} animals during the 10-min behavioral sessions (left). Either water, light, or water + light was given during a session. Light stimulation induced significantly more total number of licks (n=3, P=0.0145; two-tailed paired t-test), and licks during 3-10 min (P=0.0213; two-tailed paired t-test). **f**,**g,** Food-deprived (e, n=6) or salt-depleted (f, n=6) PKD2L1^{ChR2} mice did not exhibit appetitive behavior toward light. 300 mM NaCl or 300 mM sucrose solutions were used as control stimuli. Values are means ± s.e.m

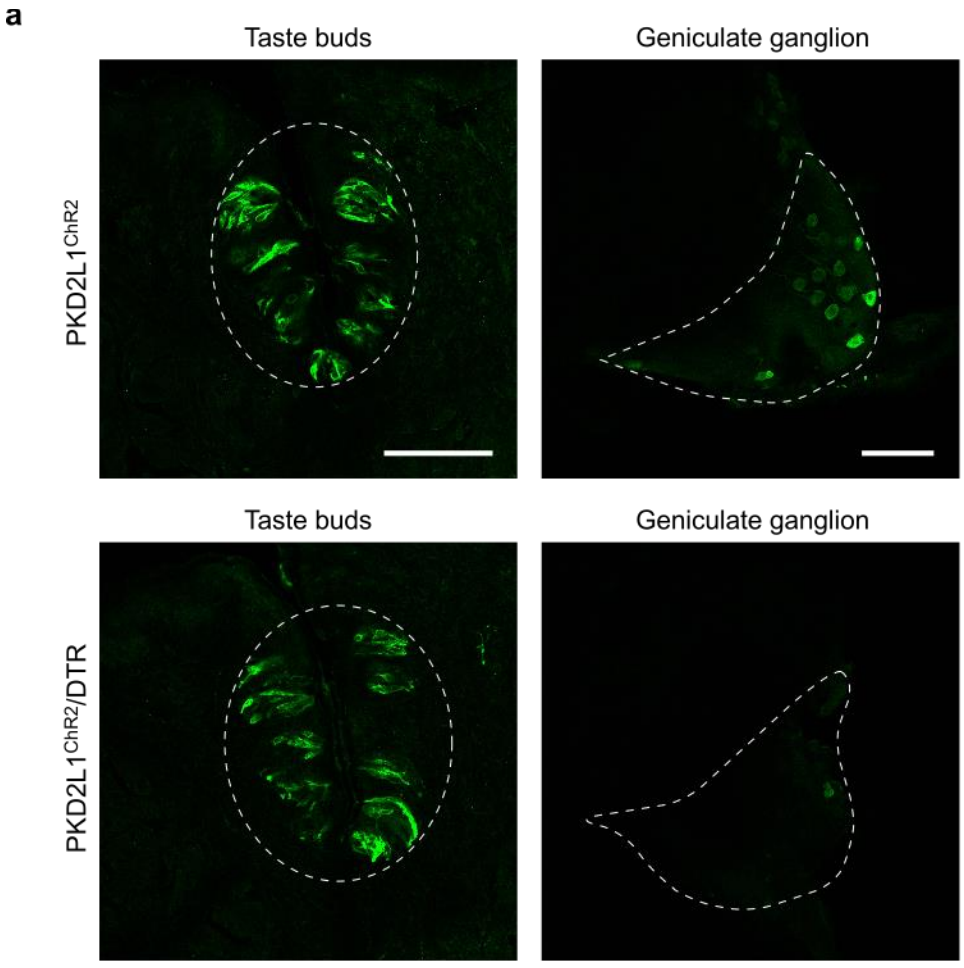
a
Taste buds
Geniculate ganglion
PKD2L1ChR2
Taste buds
Geniculate ganglion
PKD2L1ChR2/DTR

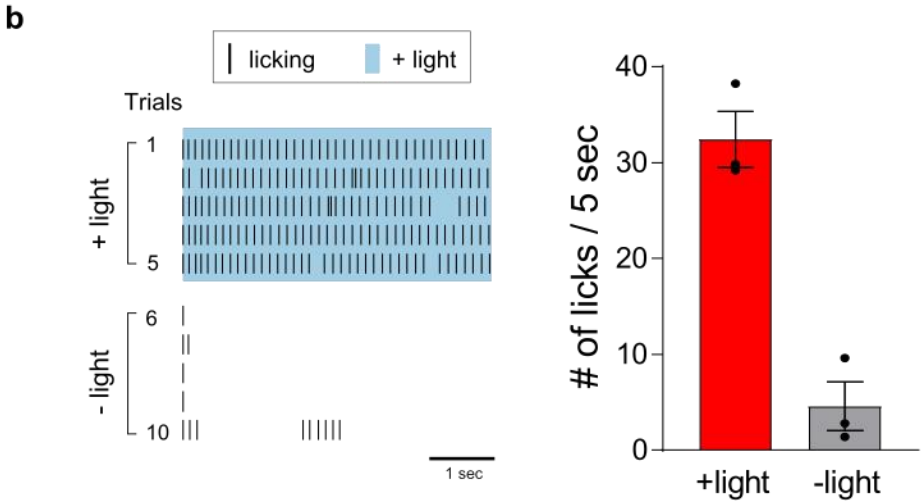
b
licking
+ light
Trials
1
5
+ light
6
10
- light
1 sec
# of licks / 5 sec
40
30
20
10
0
+light
-light

Figure 5

Figure 5: Genetic ablation of ChR2-positive geniculate neurons by diphtheria toxin. Since geniculate neurons innervate their dendrites to TRCs, ChR2-expressing geniculate population may be activated by photostimulation of the tongue. We excluded this possibility by toxin-mediated cell ablation of this population. **a**, Representative immunostaining of taste buds (left panel) and geniculate ganglia (right panel) from PKD2L1^{ChR2} and diphtheria toxin-treated animals expressing diphtheria toxin receptor in the background of PKD2L1^{ChR2} (PKD2L1^{ChR2}/DTR). After 3-4 weeks of recovery period, ChR2-EYFP expressing cells regenerated in taste buds, but not in geniculate ganglia. Scale bars, 100 μm. **b**, (left) Light-induced licking responses in a toxin-treated PKD2L1^{ChR2}/DTR animal using the same behavioral paradigm described in Figure 3b. Photostimulation of the tongue induced robust drinking (trial 1-5: blue shading) after ablation of ChR2-positive geniculate neurons. These results exclude the possibility that direct photoactivation of geniculate neurons are responsible for light-driven licking behavior. Individual black bar indicates each lick event. (right) quantification of drinking responses during 5 sec (n=3, p=0.026, two-tailed paired-t test).

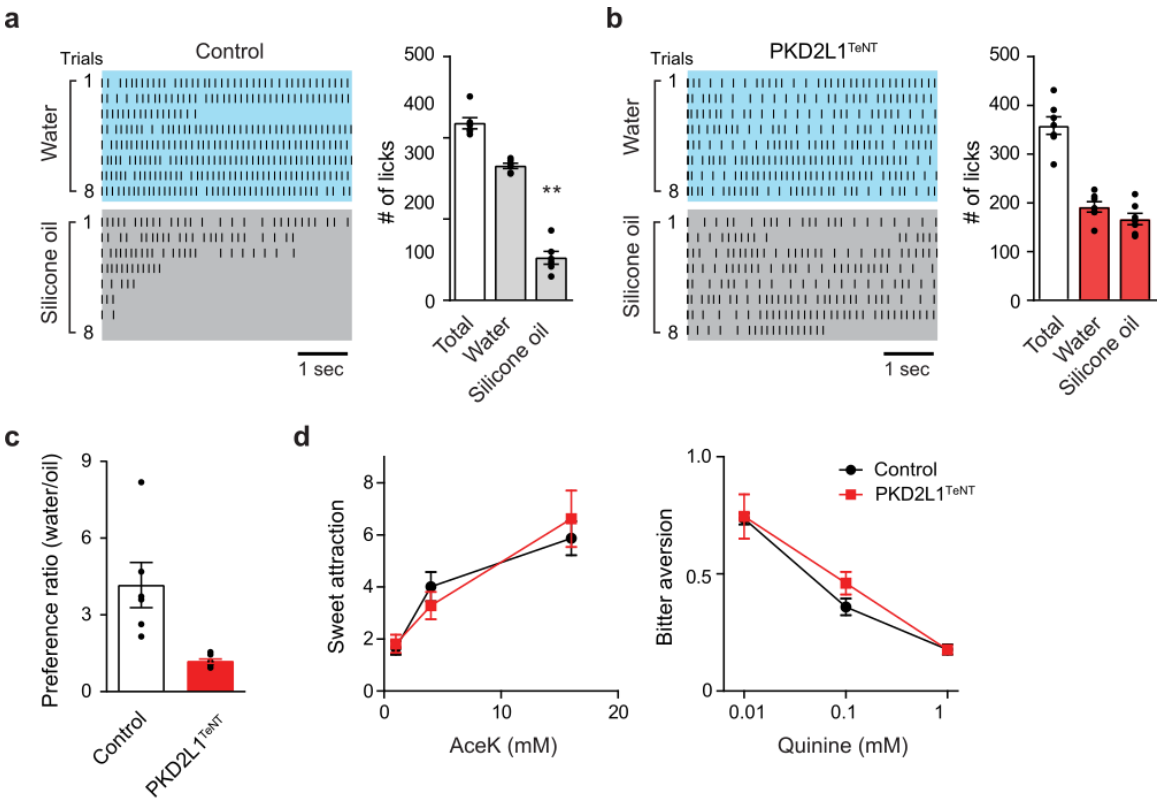

Figure 6

Figure 6: Water-induced taste signals provide a cue for fluid discrimination. a, In a brief taste preference assay, water deprived control mice (TeNT) showed strong preference toward water over silicone oil. Shown are representative licking plots toward water and silicone oil; fluids were presented for 8 times each (left). Individual black bar indicates each lick event. The number of total licks as well as licks to each fluid was quantified (right) (n=6, $p<0.0001$ for water vs silicone oil; two-tailed paired t-test). **b**, In contrast, PKD2L1^{TeNT} mice did not show preference to water and consumed the similar amount of silicone oil (n=7). **c,** Preference between water and oil was quantified as a ratio (n=7 for PKD2L1^{TeNT} and n=6 for control; P=0.0012, two-tailed Mann-Whitney U-test). **d**, both control and PKD2L1^{TeNT} mice exhibited dose-dependent attraction to sweet (AceK), and aversion to bitter (Quinine), indicating that PKD2L1^{TeNT} mice retain normal taste discrimination ability (n=4 for

PKD2L1^{TeNT} and n=6 for control). Data are show as a preference ratio to water. Values are means ± s.e.m.

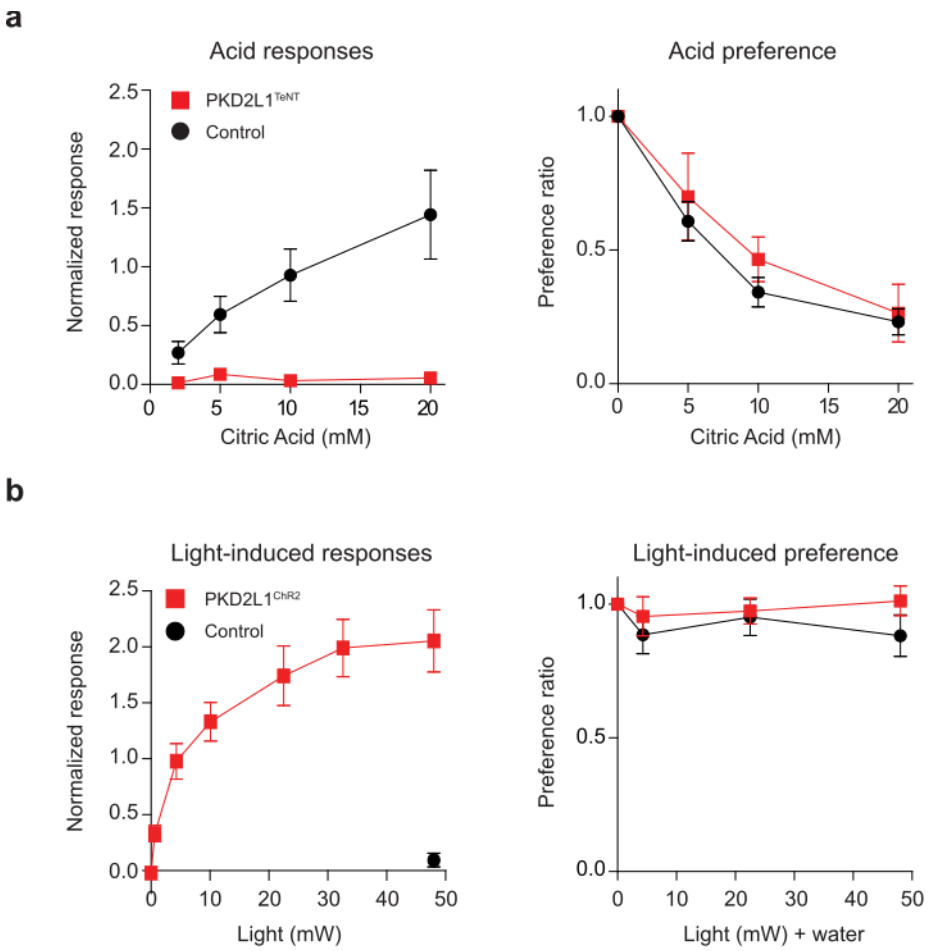

Figure 7

Figure 7: Acid-sensing taste pathway is not essential for sour aversion. a, Normalized taste nerve responses to citric acid in PKD2L1^{TeNT} and TeNT control animals (left). Control animals (n=6) show dose-dependent nerve responses to citric acid while PKD2L1^{TeNT} (n=4) mice showed no response (p=0.0095, PKD2L1^{TeNT} vs control at 20 mM citric acid). However, both PKD2L1^{TeNT} and control animals showed similar levels of aversion toward citric acid (right) (n=6 for control, and n=4 for PKD2L1^{TeNT} mice), indicating that PKD2L1-expressing TRCs are not necessary for aversive behavior to sour. **b**, Photostimulation of PKD2L1-expressing TRCs fails to induce aversion. (left) Shown are chorda tympani nerve responses to different intensities of light in PKD2L1^{ChR2} and Ai32 control animals (n=3 for

0.04-32.6mW for PKD2L1^{ChR2} mice, n=4 for the rest; p=0.0286, PKD2L1^{ChR2} vs control at 48 mW). (right) Photostimulation of PKD2L1-expressing TRCs did not change preference toward water. Mice were given a bottle containing water with an optic fiber for stimulation. Control and PKD2L1^{ChR2} mice showed undisturbed drinking behavior regardless of light intensity (n=7 for control, and n=6 for PKD2L1^{ChR2} mice). Statistical significance was analyzed with two-tailed Mann-Whitney U-test. Values are means ± s.e.m.

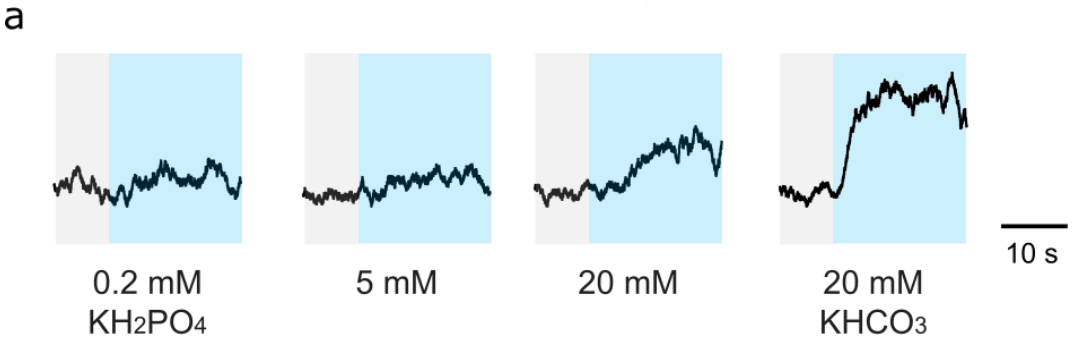

Extended Data Figure 1

Extended Data Figure 1: Ionic effects on taste responses induced by water. a, Representative water responses induced by the removal of phosphate ions. In addition to bicarbonate ions, washing out of high concentrations of phosphate (KH_2PO_4) induced minor responses.

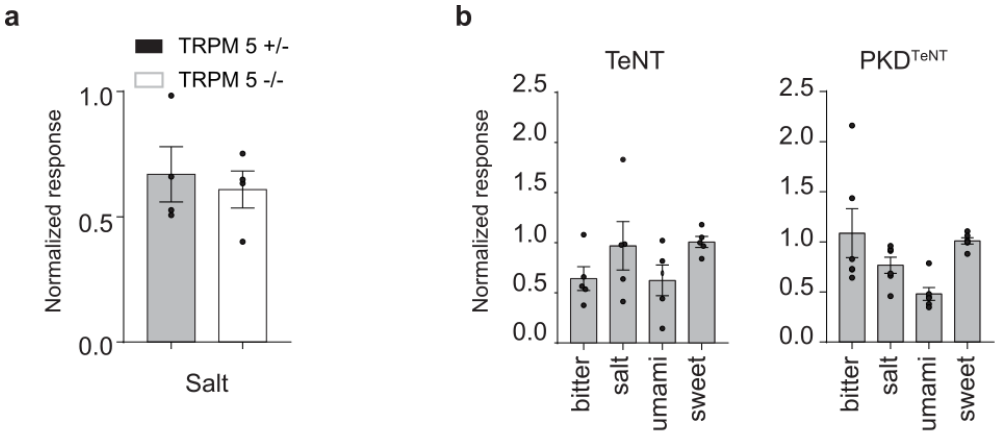

Extended Data Figure 2

Extended Data Figure 2: Taste responses in TRPM5 KO and PKD2L1^{TeNT} mice. a, Knocking out of TRPM5 has no effect on salt and sour responses. Nerve responses to salt (60 mM NaCl) in *TRPM5 -/-* mice were comparable to those in *TRPM5 +/-* control mice (n=4 for *TRPM5 -/-* and n=4 for *TRPM5 +/-*). Responses were normalized to 10 mM Citric Acid. **b**, Sour and water responses were specifically disrupted in PKD^{TeNT} mice. However, response amplitudes to bitter (0.1 mM cycloheximide), salt (60 mM NaCl), umami (50 mM MPG + 1 mM IMP), and sweet (8 mM AceK) were similar between PKD^{TeNT} (n=6) and TeNT control mice (n=5). Responses were normalized to 8 mM AceK. Data were analyzed with two-tailed Mann-Whitney U-test. Values are means ± s.e.m

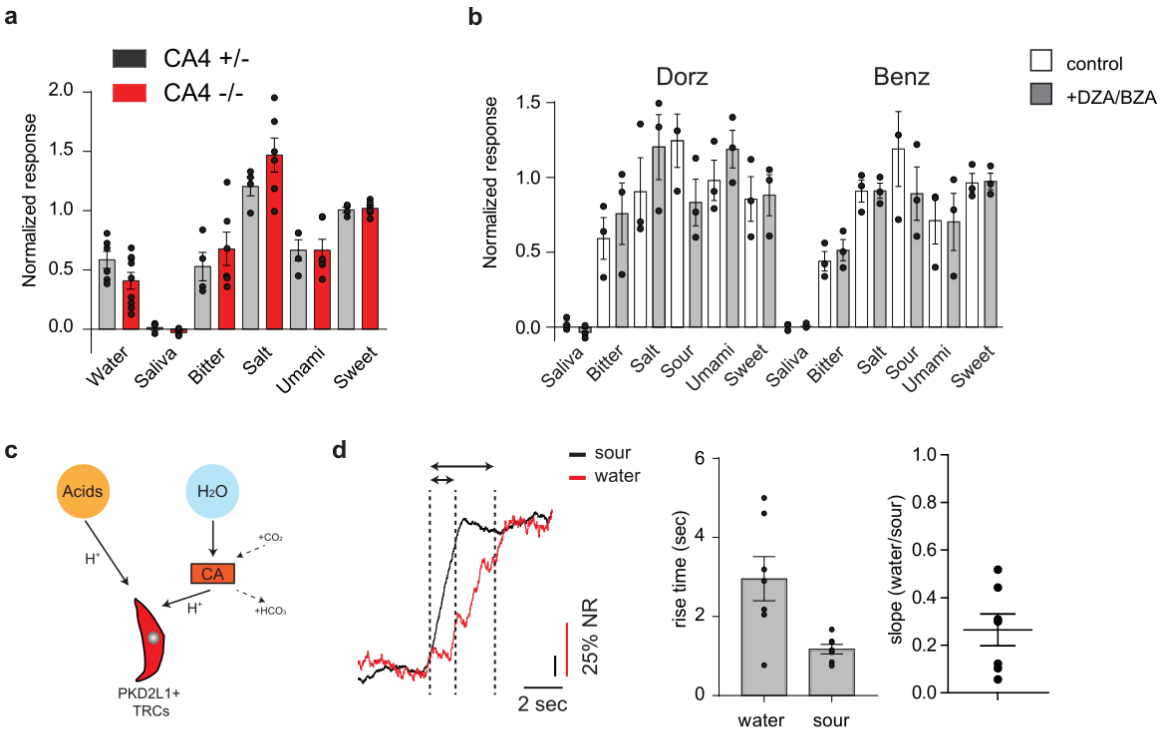

Extended Data Figure 3

Extended Data Figure 3: CA independent taste responses and the kinetics of PKD-2L1 taste responses. a, CA4 knockout mice exhibit significantly reduced responses to non-buffered water (n=9 for CA4 -/-, n=8 for CA4 -/+; p=0.0464). All other tastants evoked similar response magnitudes in both genotypes (n=6 for CA4 -/-, n=4 for CA4 +/-). **b,** Treatments with dorzolamide (DZA) or benzolamide (BZA) had no effect on basic taste responses (n=3). **c,** A proposed model for activation of acid-sensing TRCs by water and sour. Acids (protons) directly activate PKD2L1-expressing TRCs through putative proton/potassium channels.[45] On the other hand, washing out of bicarbonate with water drives catalytic reaction of CA in PKD2L1-expressing TRCs, leading to increase in local protons. **d,** Representative taste nerve responses to water and citric acid from the same animal (left). Response rise time (n=7, p=0.0157, middle), and ratio of the rising slopes (right) show slower kinetics of water responses compared to citric acid. Data were analyzed with two-tailed paired t-test. Values are means ± s.e.m

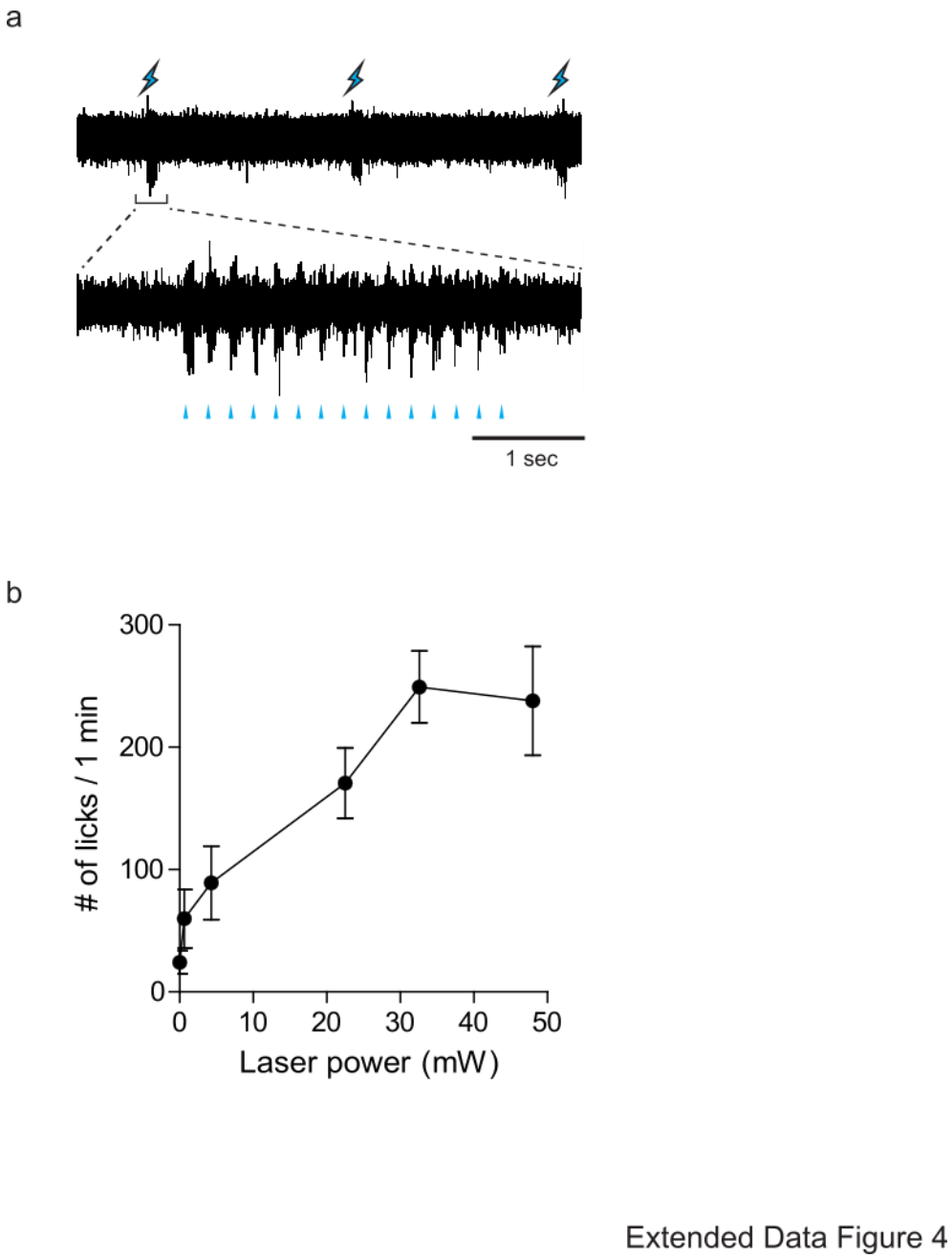

Extended Data Figure 4

Extended Data Figure 4: Light-induced taste nerve responses in PKD2L1^{ChR2} mice. a, The tongue was stimulated with laser pulses (8 Hz, 40 ms duration) at 48 mW for 2 s. Shown is a representative trace of three sets of pulse trains. Inset shows a magnified view of a 2-s stimulation window. Each blue triangle corresponds to a laser pulse. An increase in population activity in the nerve is precisely time-locked to laser pulses. **b**, Total number of

licks induced by different levels of laser power. The number of licks was summed during a 1-min session (n=5). Each data point was obtained and averaged from three PKD2L1^{ChR2} animals. Values are means ± s.e.m.

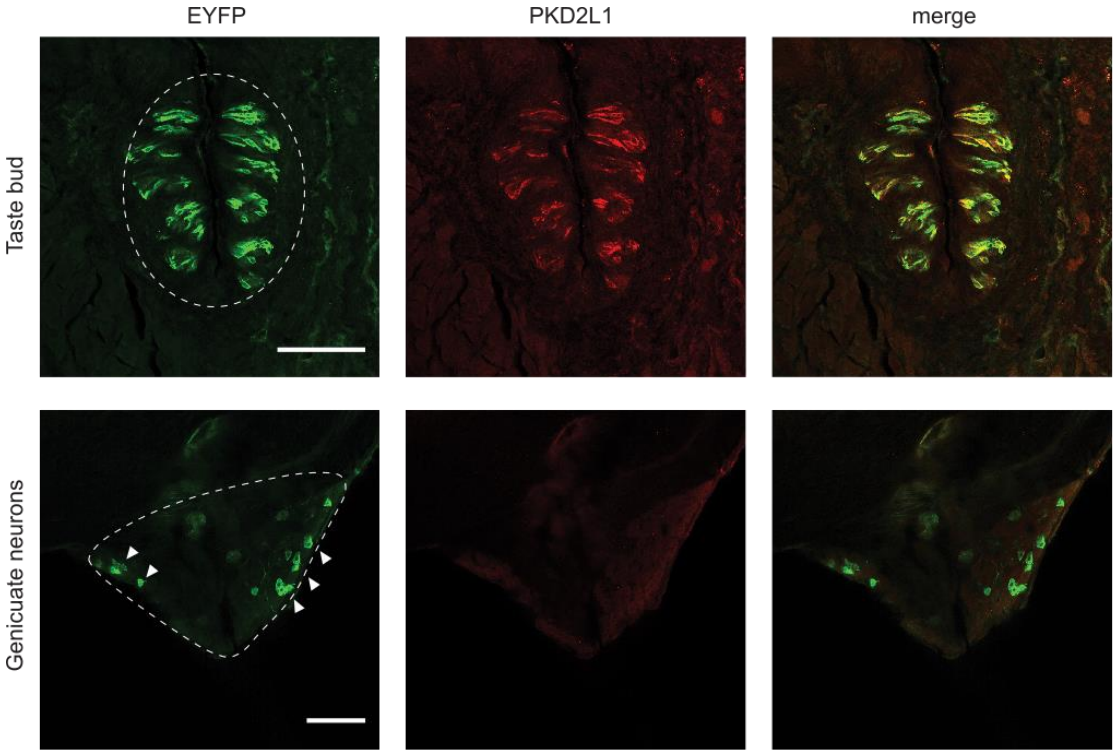

Extended Data Figure 5

Extended Data Figure 5: Ectopic expression of ChR2-EYFP in the geniculate ganglion. Tissue staining of taste buds in the circumvallate papillae (top), and geniculate ganglion (secondary taste station, bottom) from a PKD2L1^{ChR2} animal. Shown are representative staining of ChR2-EYFP (labeled with anti-GFP antibody, left), co-labeled with anti-PKD2L1 antibody (middle); the right panels show merged images. ChR2-EYFP signals overlap with PKD2L1 expression in taste buds (top panel). However, ectopic expressions of ChR2-EYFP in geniculate neurons (arrow heads, bottom left) do not show PKD2L1 expression (bottom middle). Scale bars, 100 µm.

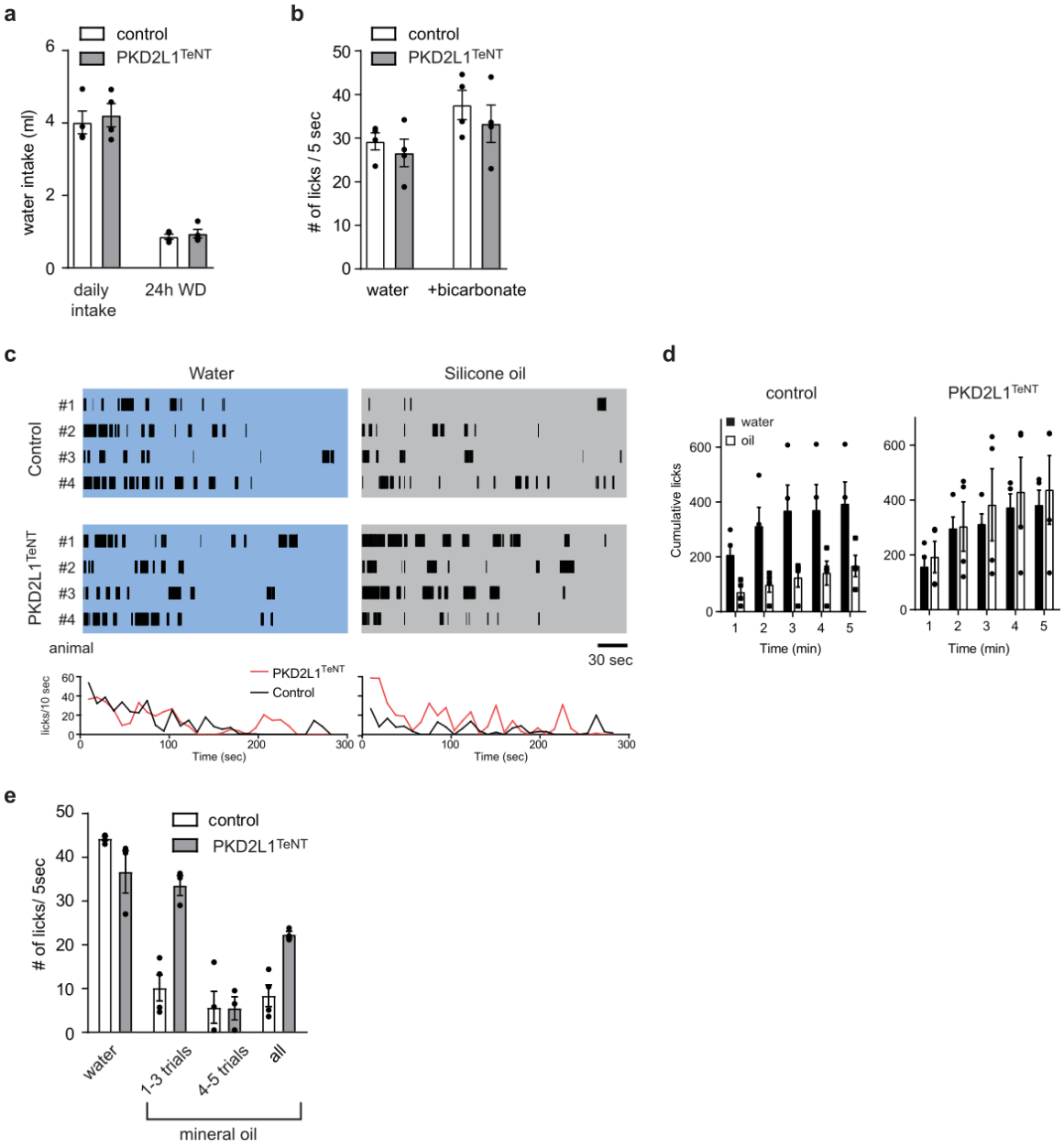

Extended Data Figure 7

Extended Data Figure 6. Acid-sensing TRCs are important for fluid discrimination, but not for water consumption. a, Spontaneous (ad-lib) and thirst-induced water intake in PKD2L1^{TeNT} and control (TeNT) mice. Both genotypes consumed similar amounts of water

(n=4 for each genotype). **b,** Water-deprived mice (24 h) exhibit no preference toward water and bicarbonate water (25 mM) which does not elicit water taste responses (n=4). These results suggest that non-taste signals are sufficient to drive animals for drinking even without water taste signals.**c,** Plots of drinking behavior of PKD2L1^{TeNT} and control mice during 5-min consumption tests. Either water or silicone oil was presented to each animal for 5 min after 23 h water-deprivation regime. Individual black bars indicate each lick event. Average number of licks are quantified for each 10-sec period (bottom). **d,** Cumulative number of licks is shown during the 5-min sessions (n=4, p=0.0188 at 5 min). **e,** A role of taste pathway for discriminating water and mineral oil. To test if animals can discriminate water and mineral oil, water was first presented to water-deprived animals for 5 s (water), followed by 5 consecutive presentations of mineral oils (5 s each, 1-5 trials). Consistent with the results of silicone oil, PKD2L1^{TeNT} initially consumed comparable amount of mineral oil to water (1-3 trials), but animals learned to discriminate in later trials (4-5 trials, n=3, p=0.0467, water vs 4-5 trials) possibly using other sensory cues such as olfaction and tactile. By contrast, control (TeNT) mice preferred water over mineral oil throughout the trials (n=4, p=0.0012, water vs 1-3 trials, p=0.0007, water vs all). Data were analyzed with two-tailed paired t-test. Values are means ± s.e.m

REFERENCES

1 McKinley, M. J. & Johnson, A. K. The physiological regulation of thirst and fluid intake. *News in Physiological Sciences: an International Journal of Physiology produced jointly by the International Union of Physiological Sciences and the American Physiological Society* **19**, 1-6 (2004).

2 Sternson, S. M. Hypothalamic survival circuits: blueprints for purposive behaviors. *Neuron* **77**, 810-824 (2013).

3 Abbott, S. B., Machado, N. L., Geerling, J. C. & Saper, C. B. Reciprocal Control of Drinking Behavior by Median Preoptic Neurons in Mice. *The Journal of Neuroscience : the official journal of the Society for Neuroscience* **36**, 8228-8237, doi:10.1523/JNEUROSCI.1244-16.2016 (2016).

4 McKinley, M. J. *et al.* The sensory circumventricular organs of the mammalian brain. *Advances in Anatomy, Embryology, and Cell Biology* **172**, 1-122 (2003).

5 Oka, Y., Ye, M. & Zuker, C. S. Thirst driving and suppressing signals encoded by distinct neural populations in the brain. *Nature*, doi:10.1038/nature14108 (2015).

6 Stricker, E. M. & Sved, A. F. Thirst. *Nutrition* **16**, 821-826 (2000).

7 Young, J. K. Hunger, Thirst, Sex, and Sleep: How the Brain Controls Our Passions. *Rowman & Littlefield Publishers, Inc.* (2012).

8 Chaudhari, N. & Roper, S. D. The cell biology of taste. *Journal of Cell Biology* **190**, 285-296, doi:10.1083/jcb.201003144 (2010).

9 Finger, T. E. Evolution of taste and solitary chemoreceptor cell systems. *Brain, Behavior and Evolution* **50**, 234-243 (1997).

10 Liman, E. R., Zhang, Y. V. & Montell, C. Peripheral coding of taste. *Neuron* **81**, 984-1000, doi:10.1016/j.neuron.2014.02.022 (2014).

11 Yarmolinsky, D. A., Zuker, C. S. & Ryba, N. J. Common sense about taste: from mammals to insects. *Cell* **139**, 234-244, doi:10.1016/j.cell.2009.10.001 (2009).

12 Chandrashekar, J. *et al.* The cells and peripheral representation of sodium taste in mice. *Nature* **464**, 297-301 (2010).

13 Shigemura, N. *et al.* Amiloride-sensitive NaCl taste responses are associated with genetic variation of ENaC alpha-subunit in mice. *American Journal of Physiology. Regulatory, Integrative and Comparative Physiology* **294**, R66-75, doi:10.1152/ajpregu.00420.2007 (2008).

14 Matsunami, H., Montmayeur, J. P. & Buck, L. B. A family of candidate taste receptors in human and mouse. *Nature* **404**, 601-604, doi:10.1038/35007072 (2000).

15 Mueller, K. L. *et al.* The receptors and coding logic for bitter taste. *Nature* **434**, 225-229, doi:10.1038/nature03352 (2005).

16 Nelson, G. *et al.* An amino-acid taste receptor. *Nature* **416**, 199-202, doi:10.1038/nature726 (2002).

17 Nelson, G. *et al.* Mammalian sweet taste receptors. *Cell* **106**, 381-390 (2001).

18 Huang, A. L. *et al.* The cells and logic for mammalian sour taste detection. *Nature* **442**, 934-938, doi:10.1038/nature05084 (2006).

19 Ishimaru, Y. *et al.* Transient receptor potential family members PKD1L3 and PKD2L1 form a candidate sour taste receptor. *Proceedings of the National Academy of Sciences of the United States of America* **103**, 12569-12574, doi:10.1073/pnas.0602702103 (2006).

20 Evans, D. R. & Mellon, D., Jr. Electrophysiological studies of a water receptor associated with the taste sensilla of the blow-fly. *The Journal of General Physiology* **45**, 487-500 (1962).

21 Wolbarsht, M. L. Water Taste in Phormia. *Science* **125**, 1248, doi:10.1126/science.125.3260.1248 (1957).

22 Cameron, P., Hiroi, M., Ngai, J. & Scott, K. The molecular basis for water taste in Drosophila. *Nature* **465**, 91-95, doi:10.1038/nature09011 (2010).

23 Liljestrand, G. & Zotterman, Y. The water taste in mammals. *Acta Physiologica Scandinavica* **32**, 291-303, doi:10.1111/j.1748-1716.1954.tb01177.x (1954).

24 Shingai, T. Ionic mechanism of water receptors in the laryngeal mucosa of the rabbit. *The Japanese Journal of Physiology* **27**, 27-42 (1977).

25 Shingai, T. & Beidler, L. M. Response characteristics of three taste nerves in mice. *Brain Research* **335**, 245-249 (1985).

26 Rosen, A. M., Roussin, A. T. & Di Lorenzo, P. M. Water as an independent taste modality. *Frontiers in Neuroscience* **4**, 175, doi:10.3389/fnins.2010.00175 (2010).

27 Edgar, W. M. & O'Mullane, D. M. *Saliva and oral health*. (British Dental Association, 1996).

28 Schneyer, L. H., Young, J. A. & Schneyer, C. A. Salivary secretion of electrolytes. *Physiological Reviews* **52**, 720-777 (1972).

29 Zhang, Y. *et al.* Coding of sweet, bitter, and umami tastes: different receptor cells sharing similar signaling pathways. *Cell* **112**, 293-301 (2003).

30 Halpern, B. P. Amiloride and vertebrate gustatory responses to NaCl. *Neuroscience and Biobehavioral Reviews* **23**, 5-47 (1998).

31 Chandrashekar, J. *et al.* The taste of carbonation. *Science* **326**, 443-445, doi:10.1126/science.1174601 (2009).

32 Boyden, E. S., Zhang, F., Bamberg, E., Nagel, G. & Deisseroth, K. Millisecond-timescale, genetically targeted optical control of neural activity. *Nature Neuroscience* **8**, 1263-1268 (2005).

33 Zald, D. H. & Pardo, J. V. Cortical activation induced by intraoral stimulation with water in humans. *Chemical Senses* **25**, 267-275 (2000).

34 Bushman, J. D., Ye, W. & Liman, E. R. A proton current associated with sour taste: distribution and functional properties. *FASEB Journal : official publication of the Federation of American Societies for Experimental Biology* **29**, 3014-3026, doi:10.1096/fj.14-265694 (2015).

35 Hanamori, T. Effects of various ion transport inhibitors on the water response in the superior laryngeal nerve in rats. *Chemical Senses* **26**, 897-903 (2001).

36 Oka, Y., Butnaru, M., von Buchholtz, L., Ryba, N. J. & Zuker, C. S. High salt recruits aversive taste pathways. *Nature* **494**, 472-475 (2013).

37 Chang, R. B., Waters, H. & Liman, E. R. A proton current drives action potentials in genetically identified sour taste cells. *Proceedings of the National Academy of*

Sciences of the United States of America **107**, 22320-22325, doi:10.1073/pnas.1013664107 (2010).

38 Dessirier, J. M., O'Mahony, M., Iodi-Carstens, M. & Carstens, E. Sensory properties of citric acid: psychophysical evidence for sensitization, self-desensitization, cross-desensitization and cross-stimulus-induced recovery following capsaicin. *Chemical Senses* **25**, 769-780 (2000).

39 Finger, T. E. *et al.* ATP signaling is crucial for communication from taste buds to gustatory nerves. *Science* **310**, 1495-1499, doi:10.1126/science.1118435 (2005).

40 Peng, Y. *et al.* Sweet and bitter taste in the brain of awake behaving animals. *Nature* **527**, 512-515, doi:10.1038/nature15763 (2015).

41 Betley, J. N. *et al.* Neurons for hunger and thirst transmit a negative-valence teaching signal. *Nature* **521**, 180-185, doi:10.1038/nature14416 (2015).

42 Baliga, S., Muglikar, S. & Kale, R. Salivary pH: A diagnostic biomarker. *Journal of Indian Society of Periodontology* **17**, 461-465, doi:10.4103/0972-124X.118317 (2013).

Chapter 2

LATERAL FLOW OF INFORMATION AT PRIMARY OLFACTORY AFFERENTS

SUMMARY

The *Drosophila* olfactory system responds to most odors with the activation of a large subset of its olfactory receptors (ORs). In contrast, a select few odors elicit responses in single ORs. In turn, these ORs are usually tuned to very few odors, a property that has been thought to be inherited by the olfactory receptor neurons (ORNs) they are expressed in. We show here that CO_2, though it activates only a single OR, actually drives activity in multiple ORN axon terminals. This activation is mediated by excitatory connections between axon terminals of the GR63a/GR21a expressing Ab1C ORN, and at least 3 other ORN types. Focusing on one of these ORNs, Ab1B, we show that the lateral inputs bypass the ORN cell bodies, only driving responses at the axon terminals. Further, we find that odor responses originating from these lateral inputs are modulated between low and high amplitude states. Finally, we show that lateral excitation is a general feature of ORN axon terminals by silencing the OR driven excitation in another ORN class, Ab1A. We find the Ab1A cell body is completely silent, while the axon terminals retain odor responses. We thus demonstrate that ORN axon terminals receive 2 sources of excitatory input, a feed-forward excitation from their OR, and a lateral excitation from other ORNs.

INTRODUCTION

The first layer of the *drosophila* olfactory pathway consists of 50 distinct classes of olfactory receptor neurons (ORNs), defined by their expression of 1 of 50 different olfactory receptors (ORs).[1,2,3] The ORN cell bodies reside in hair-like structures called sensilla that cover the 2 antenna.[4] Each sensillum houses 2-4 individual ORNs of different classes. For example, the Ab1 sensillum houses 4 ORNs: Ab1A, Ab1B, Ab1C, and Ab1D. From the antenna, the ORNs project their axons via the Antennal Nerve, to the Antennal Lobes (AL) of the brain. Here, ORN axon terminals synapse onto second order neurons called projection neurons (PNs) in small, compact structures called glomeruli. There are thus 50 glomeruli for the 50 ORN classes, defining 50 olfactory coding channels.[5,6] A typical odor binds with some affinity to a subset of the ORs, and so drives activity in multiple glomeruli. Most odors are thus represented with a combinatorial code in the AL.[7] Certain specialized odors only drive activity in single ORs, and are instead encoded in a simpler labeled line manner. For instance, cis-Vanyl Acetate (cVA) activates Or67d specifically, and is represented by a single glomerulus in the AL.[1,2,8,9,10] Similarly, CO_2 has also been shown to exclusively activate the Gr21a/Gr63a heterodimer receptor complex expressed in Ab1C ORNs.[11,12] Its representation in the AL is likewise believed to consist solely of activation of a single glomerulus, named the V glomerulus.[13]

Excitatory and inhibitory cross-talk between olfactory coding channels have been described at the PN level.[14,15,16,17,18] The excitatory interactions are mediated by excitatory local neurons[14,15,16] that connect PNs of different glomeruli via gap junctions. In contrast, only inhibitory interactions have been described between ORNs. These take the form of feed-forward inhibition of the ORN terminals[19,20,21] as well as local ephaptic effects occurring at the cell bodies.[22] Therefore, at the first layer of the olfactory pathway, excitatory responses in the 50 coding channels are thought to be completely independent of each other. In other words, tuning of any give ORN is assumed to be completely inherited from the tuning of its OR.

Here, we describe for the first time excitatory interactions between ORNs. Given its very narrow OR activation profile, we use CO_2 as a diagnostic odor for responses arising in ORN terminals via lateral interactions. Using 2-photon calcium imaging to record from all ORN axons in the AL, we identify several CO_2 responsive glomeruli. Focusing on one of these glomeruli, VA2, which gets input from Ab1B ORNs, we show that the CO_2 responses flip from a low state, characterized by a purely inhibitory response, to a high state, characterized by a strong excitation followed by a lagging inhibition. This response switch is not unique to CO_2, as we show that the same behavior occurs in Ab1B terminals in response to acetic acid. We then show that the CO_2 responses measured in the Ab1B axon terminals do not occur in the corresponding cell bodies. Instead, the excitatory component of the responses comes in laterally from Ab1C ORNs, completely bypassing Ab1B cell bodies. The inhibitory component of the responses is Orco dependent, and likely also coming in laterally. Finally, we show the presence of lateral inputs generalize to the DM1 glomerulus, which gets input from Ab1A ORNs. Here, we show multiple odors feed in laterally to Ab1A ORN terminals, again bypassing Ab1A cell bodies. We thus identify a network of excitatory interactions which allow for the lateral flow of olfactory information between ORN terminals.

MULTIPLE ORN CLASSES RESPOND TO CO_2

We began our investigation with a systematic scan through the Antennal Lobe using a pan-ORN expressing Gal4 line, pebbled-Gal4, to drive expression of GCaMP6f. Using 2-photon imaging, we probed the Antennal Lobe with 5% CO_2 and looked for responsive glomeruli. To our surprise, we measured robust responses in multiple glomeruli spanning the full depth of the Antennal Lobe (Fig1a). These glomeruli were identified by anatomical position and odor responsivity as DL1, DM1, VA2, and V. The V glomerulus corresponds to Ab1C ORNs which express the Gr63a/Gr21a heterodimer receptor-complex. This is the well characterized, CO_2 responsive olfactory channel. The other 3 glomeruli we found have not been reported as being CO_2 sensitive. Focusing specifically on VA2, we looked more carefully at the properties of these CO_2 responses. VA2 was sensitive to a narrow band of

CO_2 concentrations ranging from around 1% to 10% (Fig1b). The responses had unusually transient dynamics, consisting of a quick excitatory component, followed by a slower inhibitory period. Both inhibition and excitation scaled with the intensity of the CO_2 stimulus (Fig1b,c). These transient dynamics are in stark contrast to how VA2 responds to other odors, for example Diacetyl (Fig1e). This contrast was more pronounced for stimuli of longer duration. For 10s CO_2 pulses, VA2 responses were dominated by the inhibitory component, leading to heavily truncated excitatory responses. On the other hand, CO_2 responses in V were more typical (Fig1d,f,g). In summary, these results indicate that CO_2, a particularly narrowly activating odor as measured at the ORN cell body, activates multiple ORN axon terminals. Furthermore, the CO_2 responses are characterized by a transient excitation, riding on a strong inhibitory component.

VA2 CO_2 RESPONSES SWITCH FROM A LOW TO HIGH RESPONSIVE STATE

Having identified new CO_2 responsive glomeruli, the question arises of why these responses have not been described in the past. We investigated this discrepancy, again by looking specifically at VA2 ORN terminals. Interestingly, we found that at the beginning of a recording, VA2 responded to a CO_2 stimulus with a completely inhibitory response (Fig 2a,b). Diacetyl stimulation elicited normal responses in VA2, and CO_2 elicited robust responses in V, showing that the preparations were in good condition, and that the CO_2 stimulus was being delivered properly. By the end of the recordings, the CO_2 responses in VA2 switched to the 2 component response we described above, consisting of a full excitatory component riding on top of the slower inhibition (Fig 2a,b). Diacetyl responses in VA2 and CO_2 responses in V did not potentiate in the same way, showing that this switching effect is odor specific in VA2 for CO_2, and that it is not due to accumulation of CO_2 (Fig 2b,c).

To characterize the dynamics of this switching effect, we proceeded to deliver a CO_2 stimulus every minute for 30 minutes. We found that there is no characteristic time course for the switch: some flies switch within a few minutes, others take the full 30 minutes, and still others take over an hour (Fig 2e). Rarely, we found flies starting off in the high state (green trace Fig. 2e).

We next confirmed whether the other newly identified CO_2 responsive glomeruli also show a switching behavior. We found that indeed, each of them also switch (data not shown). Finally, we looked to see if any other odors elicit a similar switching behavior in VA2. Interestingly, we identified acetic acid as a switching odor with characteristics mirroring what we described for CO_2 (Fig2d). Together, these results show that the CO_2 responses we have characterized are modulated between a low and high responsive state. Further, this switching is not specific to CO_2, but also occurs for certain short chain fatty acids in VA2 ORNs (acetic acid, and several other related compounds for whom data is not shown).

MISMATCH IN ODOR TUNING BETWEEN VA2 ORN SOMA AND AXON TERMINALS

The VA2 glomerulus gets inputs from Ab1B ORNs, whose cell bodies reside in the Ab1 sensillum. The tuning properties of Ab1B have been well studied using single sensillum recordings (SSRs) of the Ab1 sensillum.[23] In particular, acetic acid and CO_2 responses have never been reported in Ab1B at the sensillar level. The SSR tracks the extracellular voltage in the sensillar lymph, and so is a measure for the receptor driven excitatory response of the ORN. Our results above then suggest a mismatch between the Ab1B OR, and its axon terminals. To directly confirm this mismatch, we employed SSRs of the Ab1 sensillum, and compared these recordings to 2-photon calcium imaging recordings from the corresponding Ab1B axon terminals (Fig3a). Indeed, we found that neither CO_2, nor acetic

acid elicit spiking responses in Ab1B cell bodies, while driving robust calcium responses in the corresponding terminals (Fig.3b, Extended Data Figure 1).

Given these results, there are 2 possible models for how the CO_2 responses might bypass the Ab1B cell bodies and end up in their terminals. The first model is that ORN axon terminals from some other CO_2 responsive ORN invade the VA2 glomerulus. Because we are using a pan-ORN gal4 driver to express GCaMP, we may be measuring responses from these alien terminals and erroneously attributing them to Ab1B. The second model is that the responses originate in this other CO_2 responsive ORN class, and that they input into Ab1B terminals laterally. To disambiguate between the 2 models, we tried to determine whether the responses we measured actually reside in Ab1B terminals. We expressed the beta subunit of diphtheria toxin (Dtx) in Ab1B ORNs, thereby killing this ORN class, while expressing GCaMP6f in Orco positive ORNs (Fig3Ci). Orco is a broadly expressed co-receptor required for the proper functioning of a large subset of the ORs.[24] Imaging calcium responses in this line showed that VA2 was completely silenced (Fig 3cii,iii). Therefore, no alien Orco-positive ORNs invade VA2. To determine whether Orco-negative ORNs enter VA2, we next expressed Dtx in Orco positive ORNs, while expressing GCaMP6f in all ORN types using pebbled-gal4 (Fig 3di). This manipulation allowed us to image all Orco-negative glomeruli. Once again, VA2 was completely silent (Fig3dii,iii), indicating that the CO_2 responses we measured in VA2 are not from Orco-negative ORN terminals invading VA2. Together, these results show that the CO_2 responses measured in VA2 are not from foreign terminals invading VA2, but represent signals residing in Ab1B axon terminals.

CO_2 RESPONSES IN VA2 ORIGINATE FROM ACTIVITY IN V

The data presented above supports model 2, and in particular, implies that VA2 ORN terminals receive 2 sources of excitatory input: direct excitation from the OR, and lateral excitation from some other ORN. To directly test this, we next wanted to see if VA2 CO_2 responses are independent of Ab1B OR function. We silenced Ab1B cell bodies using the

Orco mutant, *Or83b*^{2}, [24] while expressing GCaMP6f in all ORN classes (Fig.4a). In these flies, transduction potentials, and therefore, OR-mediated spiking is abolished in all Orco positive ORNs, including Ab1B. We found CO_2 responses in Ab1B terminals persisted in *Or83b*^{2} (Fig.4bi,ii). Importantly, responses in Ab1B to Diacetyl, which is known to directly drive the Ab1B OR (Fig.3b) were abolished in this line, confirming that the Ab1B OR was effectively silenced (Fig 4bi,ii). Interestingly, the dynamics of the CO_2 response were markedly different in *Or83b*^{2} compared to wild type flies. Specifically, the inhibitory component to the response was absent, with the overall response looking more like a typical, square Diacetyl response (Fig 4bi). This suggests the inhibition is Orco dependent, arising either from the Ab1B OR itself, or from some other Orco-positive ORN. In summary, the data above shows that the CO_2 responses measured in VA2 ORN terminals are not arising from Ab1B's endogenous OR, implying instead the presence of lateral excitatory inputs onto VA2 axon terminals.

The fact that excitatory CO_2 responses persist in *Or83b*^{2} also suggests that the actual source of the responses is Orco-negative. The only CO_2 responsive OR identified to date, Gr21a/Gr63a, happens to be expressed in an Orco-negative ORN class, Ab1C. We therefore hypothesized that Ab1C may be the source of the lateral excitation. To test this, we silenced Ab1C using the *Gr63a*^{1} mutant line, while expressing GCaMP in all ORN classes (Fig.4c). Surprisingly, excitatory CO_2 responses in Ab1B ORNs were abolished in the mutant, while Diacetyl responses remained (Fig 4di,ii). CO_2 responses in Ab1C were also gone, confirming that Ab1C ORNs had been effectively silenced. Interestingly, while the excitatory component to the Ab1B CO_2 responses was completely absent, the inhibitory component persisted (Fig 4di), reconfirming that the inhibitory component is genetically separable from the excitatory. Altogether, these results show that the excitatory CO_2 signals measured in Ab1B axon terminals originate in Ab1C from Gr63a/Gr21a mediated spiking.

If silencing Ab1C abolishes Ab1B CO_2 responses, artificially inducing spiking in Ab1C should lead to corresponding responses in Ab1B. We therefore expressed the light activated ion channel, CsChrimson, in Ab1C ORNs and drove GCaMP expression in Orco-positive

ORNs (Fig.4e). We imaged Ab1B axon terminal calcium responses while directly stimulating the Antenna with red light. We measured light-driven calcium responses in Ab1B terminals (Fig 4fi,ii). The responses consisted of a short excitatory phase with no inhibitory component, reconfirming that the inhibition seen with CO_2 stimuli does not originate from Ab1C. Furthermore, the light driven responses mirrored the CO_2 responses in that they switched on over the course of the recordings (Fig 4g).

DM1 ORNS ALSO RECEIVE LATERAL INPUTS

We next asked whether lateral excitatory interactions are unique to CO_2, or whether they generalize to other odors in other glomeruli as well. We began by constructing an odor tuning panel in another ORN class, Ab1A, projecting into the DM1 glomerulus. We measured the tuning at the level of the Ab1A cell bodies using SSRs, and at the level of their axon terminals using 2 photon imaging of DM1 (Fig.5a). Interestingly, we found some discrepancies between the tuning panels, with the terminals responding to odors to which the cell bodies did not (Fig 5b). Some odors showed stronger responses at the terminals than in the cell bodies, while others showed slightly higher responses in the cell bodies than in the terminals. These last odors tended to be broadly activating, strong stimuli likely recruiting feed-forward inhibition.[14,15,16]

To determine whether any of the DM1 odor responses originated from lateral inputs, we next eliminated OR-mediated excitation of Ab1A by silencing its OR with the *Or42b*^{2} receptor mutant. Again, we recorded spikes at the cell body and calcium at the axon terminals (Fig.5c). Intriguingly, Ab1A cell body responses collapsed completely in the receptor mutant, while terminal responses largely persisted (Fig 5d, Extended Data Figure 2). The only odor to which Ab1A axon terminals lost their responses was dilute Ethyl Acetate, an odor known to very specifically activate only Ab1A when presented at sufficiently low concentrations.[25,26] Where do these residual responses arise from? To answer this, we repeated this experiment in the *Or83b*^{2} line used above (Fig.5e). Silencing Orco-positive ORNs silences a large subset of the entire ORN population. As expected, we

found that all Ab1A cell body responses were abolished, and additionally, all Ab1A axon terminal responses collapsed as well, with the exception of CO_2 (Fig 5f). This suggests that the residual terminal responses (Fig.5d) are the result of lateral inputs from other Orco-positive ORNs onto Ab1A terminals.

Finally, we addressed the possibility that we may have misidentified DM1 in the imaging experiments. To confirm the correct identification of DM1, we expressed Dtx in Or42b positive ORNs while expressing GCaMP in all ORNs. DM1 was noticeably absent from the baseline fluorescence in these flies, and all Ab1A axon terminal odor responses were absent (Extended Data Figure 3). This confirmed that we correctly identified DM1 in the imaging experiments. Together, these results suggest that most odors activating DM1 arise from both direct activation of Ab1A cell bodies as well as indirect, lateral excitatory inputs from other ORN classes, most of which are Orco-positive. Lateral excitatory inputs thus seem to be a general feature of ORNs in the AL circuit.

MIXED EXCITATION AND INHIBITION CONFERS SPECIAL RESPONSE PROPERTIES ON ORN AXONS

We have shown that the inhibitory component to the VA2 CO_2 response is Orco dependent (Fig.4bi,ii). DM1 CO_2 responses also have an inhibitory component (Fig.5b). Moreover, this inhibition is not coming from the Ab1A OR, that is, it is not a consequence of direct suppression of the Ab1A OR, as it persists in the *Or42b*^{2} fly (Fig.5d). Like for VA2, however, the inhibitory component disappears in the *Or83b*^{2} fly (Fig.5f). Therefore, it seems likely that the inhibitory component to the DM1 CO_2 responses are coming in through lateral inhibitory inputs originating from Orco-positive glomeruli. Inhibition, together with lateral excitation, thus seems to be a general feature of CO_2 responses in VA2 and DM1.

What capabilities might the interplay of lateral excitation and inhibition confer to the axon terminals of these glomeruli? To investigate this, we probed the dynamics of the CO_2 responses in these glomeruli by presenting either tonic or pulsed CO_2 stimuli. Focusing first on VA2, we presented a tonic CO_2 stimulus for 15s and measured a transient excitatory response which was quickly overwhelmed by the inhibitory component (Fig.6a, top panel first column, also see Fig.1d). The same amount of CO_2 pulsed at 1Hz for 30s at a 0.5 duty cycle led to 30 individual excitatory peaks riding on top of a slowly growing inhibitory component (Fig.6a, top panel, second column). In contrast, VA2 responded to tonic stimulation with Ethyl Butyrate, an odor known to drive activity at the Ab1B OR (Fig.3b), with a more typical square pulse, and responded to pulsed Ethyl Butyrate with 30 excitatory peaks (Fig.6a, top panel, third and fourth columns). In other words VA2 was able to precisely follow and represent the Ethyl Butyrate odor stimuli whether they were pulsed or prolonged. On the other hand, it was able to follow pulsed CO_2 stimuli, or only the onset of more prolonged stimuli. The VA2 PNs matched the behavior of the ORNs (Fig.6a, bottom row). We then repeated the same experiments for DM1, and found the same general phenomenon (Fig.6b). Together, these results suggest that the interplay of lateral excitation with inhibition cause VA2 and DM1 to selectively encode the onsets of prolonged CO_2 stimuli.

DISCUSSION

We began by mapping the glomerular representation of an odor known to be particularly selective at the receptor level. CO_2 has only been shown to activate the Gr63/Gr21 receptor complex expressed in Ab1C ORNs. Here, we have shown that the CO_2 representation broadens significantly at the level of the ORN axon terminals, eliciting responses in multiple gomeruli. These responses switch from a low to high activity state, with the low state being characterized by a purely inhibitory response, and the high state consisting of both excitation and inhibition. This switching likely accounts for these glomeruli not having been identified as CO_2 responsive up until now. While the underlying mechanism is unclear, it seems likely the switching represents changes in the animal's internal state.

However, coarse manipulations of internal state including starvation, feeding, inducing stress, and exposure to heat or cold, did not bias the flies to be in the high or low state (data not shown). Yet neuromodulation of the ORN terminals is not without precedent,[36] suggesting that some similar mechanism may be involved. Further work aiming to connect the switching of CO_2 responses to the animals' behavioral state will no doubt help elucidate the precise relationship between the two.

In investigating the sources of these new CO_2 responses, we first noted the unique dynamics of the CO_2 responses in VA2 as compared to other ligands. The responses were characterized by a period of excitation followed by inhibition. The excitation and inhibition were genetically separable, with the excitation being Gr63a-dependant, and the inhibition being Orco-dependant. The interaction of excitation and inhibition led to the overall excitatory response being very short, presumably corresponding to a very transient release of neurotransmitter at the ORN-PN synapse. This overall effect was recapitulated in DM1 as well. We found that the transient nature of the CO_2 responses allows these glomeruli to emphasize the onset of a CO_2 stimulus while ignoring the overall duration of the stimulus. It is particularly notable that this filtering of odor responses happens selectively for CO_2 over other odors in both glomeruli. Ethologically, transient CO_2 responses might be useful in tracking CO_2 odor plumes, as a way of emphasizing when the animal enters and leaves the plume.

Interestingly, activation of DM1 and VA2 has been associated with attractive, food signaling odors[30]. Furthermore, Ab1A and Ab1B ORNs projecting to these glomeruli, drive strong, attractive behavioral responses when optogenetically activated.[31] We thus have 2 glomeruli associated with behavioral attraction which seem to be tuned to the onset of CO_2 stimuli, and inhibited by long CO_2 pulses. CO_2 is a behaviorally interesting odor stimulus. It has been well established that CO_2 can elicit aversive behavioral responses in simple T maze assays,[11,32,33] and that this aversion is mediated by activation of the V glomerulus.[32,33] Indeed, sufficiently high concentrations of CO_2 can be deadly. On the other hand, CO_2 is a natural byproduct of fermentation processes occurring on the preferred food source of

drosophila: rotting fruit. It would therefore be present in olfactory stimuli corresponding to food sources, clearly an attractive stimulus. Interestingly, recent evidence has shown that CO_2 can drive robust behavioral attraction under certain circumstances.[28,29] In the case of the first paper, the behavior is modulated in a circadian manner, tracking the periods of highest activity during the day. In the case of the second study, the attraction seems to be linked to flight. It therefore seems that CO_2 is able to act as either an aversive or attractive stimulus given the proper context. Our physiological results fit into this model by providing one possible neural substrate for *drosophila*'s response to a CO_2 stimulus: the relative balance of attraction from VA2/DM1 and aversion from V. The fact that the responses in VA2 and DM1 not only favor shorter CO_2 stimuli, but also undergo a switch from low to high states suggest that this balance is delicate and favors certain CO_2 dynamics at certain times.

We found that CO_2 elicits responses in the Ab1B axon terminals, but not the corresponding cell bodies. The terminal responses originate from Ab1C, which appear to completely bypass the Ab1B cell bodies and input to their axon terminals instead. This result generalizes to Ab1A terminals in DM1, which also receive massive lateral inputs. Indeed, silencing Ab1A cell bodies has little effect on the responsiveness of the corresponding axon terminals. One interesting feature of the AL circuitry is a broadening of odor tuning in PNs compared to their cognate ORNs.[35] This has been attributed to a combination of a particularly strong ORN to PN synapse, as well as electrical excitatory interactions between PNs of different glomeruli, and lateral pre-synaptic inhibition. These factors together serve to make the PNs more sensitive to odors which only weakly activate their cognate ORNs. Increasing the number of coding channels being used for any given odor is thought to contribute to an overall increase in the efficiency of odor coding. Our results, then, suggest another mechanism by which ORN to PN broadening of odor tuning may occur; namely, broadening at the ORN axon terminals themselves, by lateral excitatory connections.

METHODS

Flies

Experiments were done on female flies 5-20 days post eclosion, with the exception of the *ShakB* genotype, for which males were used. The following genotypes were used for each figure:

Fig. 1,2 : pebbled-gal4,uas-opGCaMP6f

Fig. 3 (B): Or42b-gal4/uas-Cβ-DT.I ; Or83b-lexA,lexAop-opGCaMP6f (C): uas-Cβ-DT.I/+ ; Or92a-gal4/Or83b-lexA,lexAop-opGCaMP6f (experimental), +/SM6 ; Or92a-gal4/Or83b-lexA,lexAop-opGCaMP6f (no DT.I control) (D): pebbled-gal4,uas-opGCaMP6f ; ; Or83b-lexA/lexAop- Cβ-DT.I (experimental) pebbled-gal4,uas-opGCaMP6f ; ; lexAop-Cβ-DT.I (no lexA control).

Fig. 4 (B): pebbled-gal4,uas-opGCaMP6f ; ; Or83b[2] (experimental), pebbled-gal4,uas-opGCaMP6f ; ; Or83b[2]/MKRS (het control) (D): pebbled-gal4,uas-opGCaMP6f ; ; Gr63a[1] (experimental), pebbled-gal4,uas-opGCaMP6f ; ; Gr63a[1]/MKRS (het control) (F,G): uas-CsChrimson-mVenus/SM6;Gr21a-gal4/Or83b-lexA,lexAop-opGCaMP6f

Fig. 5 (B): uas-Cβ-DT.I/+ ; Or92a-gal4/Or83b-lexA,lexAop-opGCaMP6f (D): pebbled-gal4,uas-opGCaMP6f;Or42b[2] (F): pebbled-gal4,uas-opGCaMP6f ; ;Or83b[2]

Fig. 6 pebbled-gal4,uas-opGCaMP6f (ORNs), GH146-gal4;uas-opGCaMP6f (PNs)

Odor Delivery

Odor stimuli were delivered via an olfactometer setup. Briefly, a carrier stream of breathing air was directed through a mass flow control (MC-2SLPM-D), into a carrier tube, and to the fly. Another stream of breathing air was directed through a separate mass flow control, into a 3-way solenoid valve (Asco Valve 411-L-1324-HVS) with the normally open output connected to a solvent vial (paraffin oil or water), and the normally closed output connected to an odor vial. Both odor and solvent vial outputs were then connected to the carrier tube to join the carrier airstream to the fly. For CO_2 stimuli, the olfactometer was modified by adding another solenoid valve. Carrier air was delivered as above. A second mass flow controller directed breathing air through a ‘balance’ valve with the normally open output connected to the carrier, and the normally closed output venting outside the microscope

box. A third mass flow controller directed CO_2 through a 'CO_2' valve, which had the normally open output venting outside the microscope box, and the normally closed output connected to the carrier tube. Both CO_2 and balance valves were driven by the same TTL pulse, and both CO_2 and balance mass flow controllers were set to the same flow rates, so that when the balance was inputting to the carrier, the CO_2 was venting outside the microscope box, and when the CO_2 was inputting to the carrier, the balance was venting outside the box. In this way, we kept a constant total flow rate to the fly, TTL Low: carrier flow rate + balance flow rate, TTL High: carrier flow rate + CO_2 flow rate.

All odor stimuli consisted of a 3-second odor pulse delivered 10 seconds into a 30-second trial, except for figure 1d, where the odor pulses were 10 seconds, and figure 6, where CO_2 was either pulsed at varying frequencies for a total of 30 seconds, or presented in a 15s long pulse.

Total airflow to the fly was always 200 mL/min, except for recordings from figure 4c, and figure 6, where the total flow rate was 2000 mL/min. In figure 6, the flow rate was increased so as to minimize the latency to response to the pulsed CO_2 stimuli, allowing the accurate capture of high frequency responses in the ORN and PN terminals. In figure 4C, the flow rate was increased so as to have the odor stimuli onset better match the near zero latency light stimulus.

Odor stimuli are presented as the concentration arriving at the fly (after dilution in the carrier air stream). The ratio of odor/solvent to carrier flow rates was used to dilute odors.

Calcium imaging of odor evoked signals

The antennal lobe was exposed, and subsequently imaged dorsal side up using a 2-photon laser scanning microscope. The frame rate was set to 5.5 fps for every recording, at a resolution of 224x224 pixels. Oxygenated saline was perfused into the imaging chamber throughout the recordings. PMT filters used were a 525nm with 50nm bandwidth, except for optogenetic experiments, where a 500nm with 20nm bandwidth filter was used (Newport, HPX500-20).

Calcium imaging of optogenetically evoked signals

The same preparation was used as described above, with the same resolution and frame rates. Odor stimuli consisted of 3-second pulses, coming on 10 seconds after the start of the trail. Light pulses consisted of a 1-second pulse of light, coming on 10 seconds after the odor pulse, that is, 23 seconds after the onset of the trial. Light stimuli were delivered through a fiber optic cable coupled to a 625nm LED (ThorLab M625F2). The fiber optic was positioned under the fly antenna to mimic the odor stimulation. The use of the 500nm filter PMT filter described above allowed for simultaneous stimulation with red light while still imaging GCaMP signals in the antennal lobe.

Single Sensillum Recordings

Flies were mounted onto an electrophysiological rig setup. Briefly, female flies were immobilized by pushing them into a pipette tip, with the very end cut off. The head of the flies was thus exposed, while the rest of the body was stuck in the tip. Hooks made out of glass capillary tubes (World Precision Instruments TW150f-3) were used to stabilize the antenna. Ground and recording electrodes consisted of AgCl coated silver wire inserted into saline filled sharp pipettes, also pulled from glass capillary tubes. The ground and recording pipettes were inserted into the eye, and Ab1 sensilla, respectively. Signals were acquired with a MultiClamp 700B amplifier low pass filtered at 2 kHz and digitized at 10kHz. Odor/light stimuli were delivered as described above.

Imaging Analysis

dF/F was calculated as $(F-F_0)/F_0$, where F was the mean pixel intensity in a given ROI, and F_0 the baseline in the same ROI, defined as the mean pixel intensity in the 10 seconds prior to the onset of the odor stimulus. Prior to the dF/F calculation, F was baseline subtracted to correct for any ambient light or excessive PMT noise. This consisted of subtracting from every element in the time series, F, the pixel intensity at the same time point in an equally sized ROI in the background (area with no GCaMP signal).

For the heatmaps, dF/F was calculated for each pixel in the image, at the peak of the odor response (average of the 3 frames centered on the response peak). The resulting images from 3 separate presentations of the odor were then averaged. This averaged image was

thresholded to remove stray pixels with large transient dF/F values, and subsequently convolved with a Gaussian filter to produce the final images. For display in the main figures, the boundary of the antennal lobes was traced, and the region outside the lobes was blacked out.

Electrophysiology Analysis

Spikes were sorted by amplitude using a custom script in MATLAB. Where needed, Ab1A or Ab1B were selectively ablated so as to unambiguously identify either the B or A spike (figures 3, 5 respectively). Peristimulus time histograms (PSTHs) were calculated from the spike sorted data (50ms bins overlapping 25ms). For purposes of display, the PSTHs were baseline subtracted such that the resting spiking frequencies were all close to zero.

Fly Rearing

Flies were reared on standard diet and kept at 25°C in a 12:12 light to dark cycle. For optogenetic experiments, flies were additionally reared in their standard diet plus the addition of potato flakes, hydrated with 140□M all-trans-retinal in H_2O.

Getting CO_2 responses

Excitatory CO_2 responses in VA2 and the other newly responsive glomeruli emerge over the course of a recording. This switching is captured by repeatedly probing the relevant glomeruli with CO_2 stimuli over time (fig 2D). For figure 2A-C, a diacetyl stimulus was given, followed by a CO_2 stimulus (beginning). VA2 responses were then probed every 10-20 minutes with CO_2, until the excitatory responses developed. Once the excitatory response stopped growing, a final CO_2 stimulus was delivered followed by diacetyl (end). The switching process took anywhere from 10 minutes to an hour (fig 2D). Rarely, a fly might start out responding to CO_2 upon first presentation (black trace in fig 2D). A similar protocol was followed in figure 2E, using acetic acid instead of CO_2.

For the sensillum recordings in figure 3A, the flies were left on the rig for a similar amount of time as their counterparts in the 2 photon imaging experiments of the same figure. This was done to allow for any potential switching of the CO_2 response at the Ab1B cell bodies. In figure 4B, Gr63a mutant flies were probed with CO_2 for a similar amount of time as the heterozygote controls were, again to allow for any potential switch in VA2. A subset of

Gr63a mutants were left on the imaging rig for up to 2 hours to account for the possibility that the mutation may simply delay the switching behavior. No excitatory responses were ever recorded. For figure 4C, VA2 was probed with light and CO_2 stimuli at various time points until the excitatory responses emerged. This usually happened first for CO_2, shortly followed by light.

Acknowledgements

We thank M. Meister, M. Dickinson, and P. Sternberg for helpful comments, and D.J. Anderson for uas-opGCaMP6f flies. We particularly acknowledge M. Dickinson and F. Van Breugel, whose prior work showed that CO_2 can elicit reliable attractive behavior, and uncovered Ir25a as a novel CO_2 responding olfactory receptor. It was this work that led us to look at CO_2 responses in the antennal lobe.

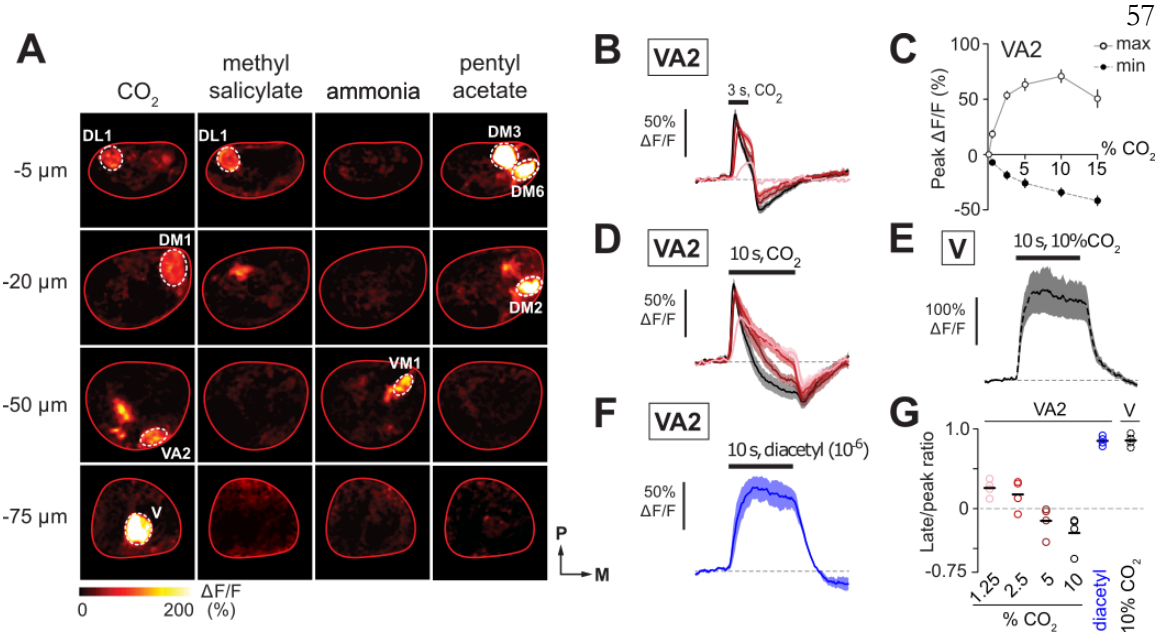

Figure 1: CO_2 elicits responses in multiple glomeruli of the antennal lobe. a, Representative images from a single experiment showing CO_2 responsive ORN terminals in Pb-Gal4,uas-opGCaMP6f. Each column represents a different odor stimulus, each row a different depth in the antennal lobe (in µm). Panels arranged dorsal to ventral from top row to bottom. Odors were selected to accurately identify each imaging plane. CO_2 responsive glomeruli were identified by location and odor tuning as DL1, DM1, VA2, and V (from top to bottom). Odor concentrations were: 5%CO_2, 5x10^{-6} pentyl acetate, 10^{-3} NH_4, 10^{-6} methyl salicylate. **b,** Average dF/F time courses in VA2. Responses are to increasing concentrations of 3s CO_2 pulses (n=3-9). **c,** Quantification of maximum and minimum peaks of the CO_2 responses in B. **d,** Average dF/F time courses in VA2 in response to 10s pulses of CO_2 at varying concentrations (n=4). **e,** Average VA2 responses to a 10s pulse of 10^{-7} diacetyl (n=4). **f,** Average responses in V, to a 10s, 10% CO_2 pulse (n=4). **g,** Quantification of late to peak amplitude ratios for the 10s stimuli. Late response amplitude defined as response amplitude 8s after peak response. Envelopes in average time courses, and error bars are SEMs.

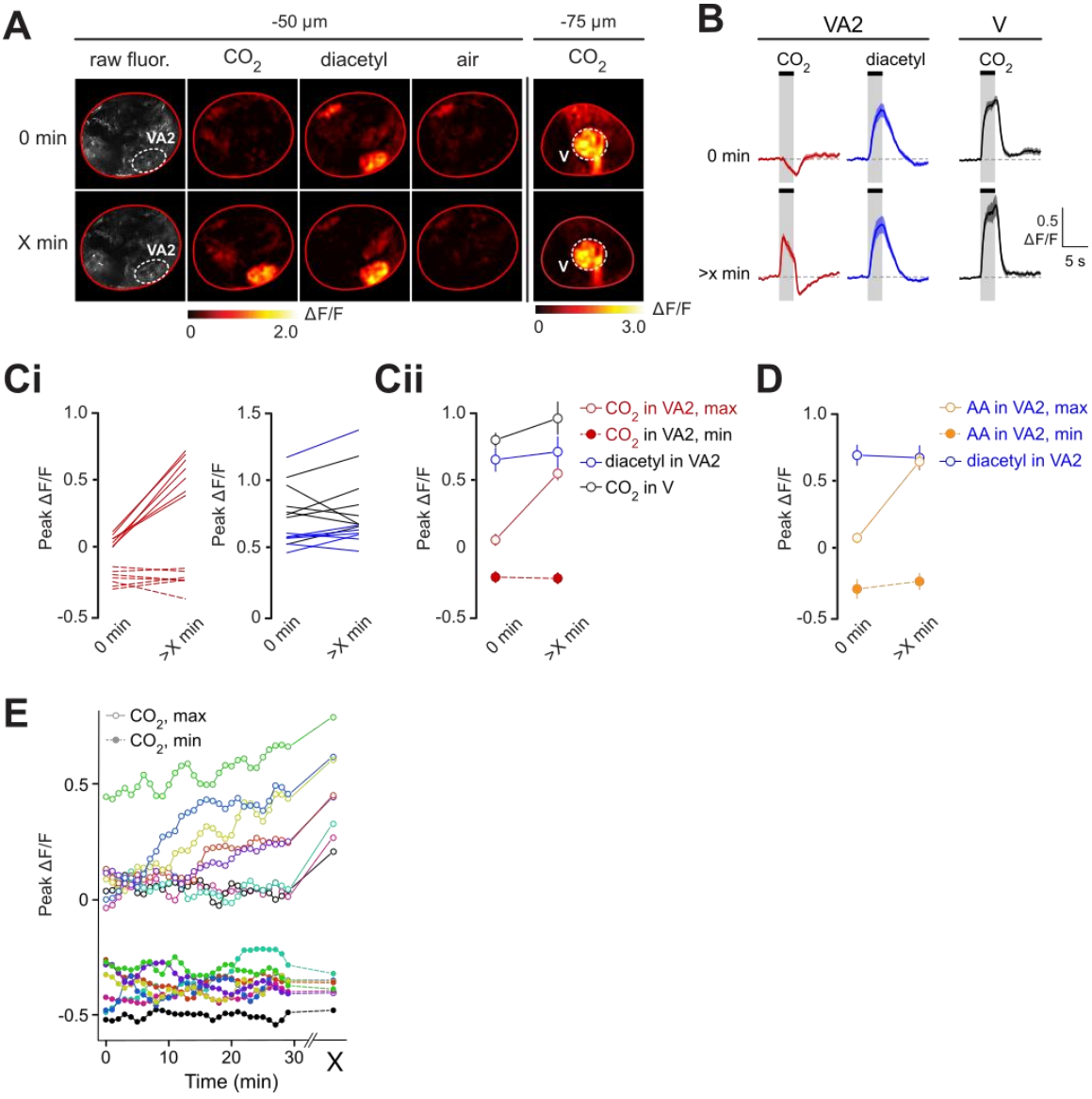

Figure 2: CO_2 responses switch from a low to a high state over the course of a recording. a, Representative images from a single experiment showing example responses to 5% CO_2 (in VA2 and V), 10^{-7} diacetyl, and breathing air (in VA2). Top row shows responses measured at the start of the experiment, bottom row shows responses in the same plane at the end of the experiment. Time between beginning and end of the experiment was approximately 15 minutes for this recording. Note absence of excitatory CO_2 responses in VA2 at the beginning and presence at the end, as well as no changes in diacetyl or V glomerulus CO_2 responses. **b,** Average dF/F time courses in response to 5% CO_2 (red, in

VA2, black, in V) and 10^{-7} diacetyl (r=blue, in VA2) at the beginning and end of experiments (n=7). VA2 responses to CO_2 at the beginning of the experiments represent the low state, characterized by a purely inhibitory response. VA2 responses by the end of the experiments represent the high state, consisting of a large excitatory component, overlaid on the inhibition. **c,** Quantification of data in B, maximum and minimum peaks for CO_2 in VA2, and maximum peaks for diacetyl in VA2, and CO_2 in V. Individual data points are plotted in Ci, averages are plotted in Cii (same color code as in B). **d,** Quantification of switching behavior in VA2 in response to acetic acid. Plotted are average values of maximum and minimum peaks for 1.5% acetic acid (yellow), and maximum peaks for 10^{-7} diacetyl (blue) (n=4). **e,** Time courses of the CO_2 switch from low to high states in VA2. 10% CO_2 was delivered every minute for 30 minutes. Plotted are both peak excitatory (open) and inhibitory (closed) responses to CO_2 presentations in 7 representative animals. Note the varying time course of the switch, as well as the constant amplitude of the inhibitory peaks. Envelopes in average time courses, and error bars are SEMs.

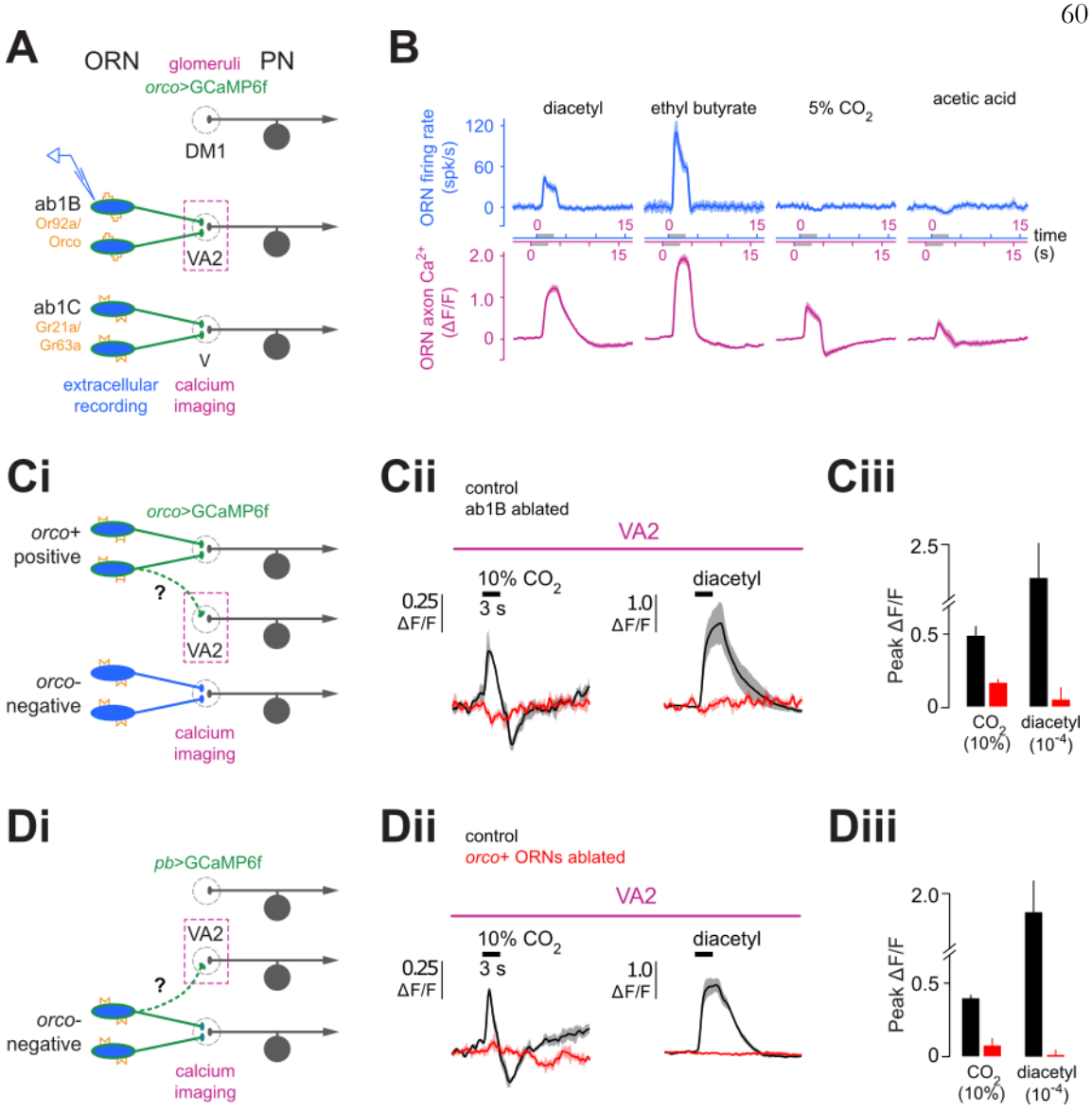

Figure 3: Mismatch in odor tuning between Ab1B cell bodies and axon terminals. a, Schematic showing experimental setup. Extracellular single sensillum recordings (SSRs) are made from Ab1 sensilla, and compared to 2-photon calcium responses in VA2. Recordings are done with Ab1A (DM1) ablated for ease of spike identification. GCamP6f is expressed under the control of Orco-lexA, and diphtheria toxin (dtx) is under the control of Or42b-gal4. **b,** Peristimulus-time-histograms (psths) from SSRs (blue, top row) compared to corresponding average dF/F timecourses from imaging experiments (purple, bottom row). Note absence of CO_2 and acetic acid responses in Ab1B cell bodies. Odor

concentrations were: 5% CO_2, 1.5% acetic acid, 10^{-7} diacetyl, 10^{-5} ethyl butyrate (n=3-5 for imaging, n=4-6 for SSRs). **c,** CO_2 responses in VA2 are not from foreign orco-positive terminals invading VA2. GCaMP6f is expressed under control of orco-lexA, and Ab1B ORNs are ablated by expressing dtx under control of Or92a-gal4. Responses in VA2 are recorded using 2-photon imaging (Ci). Average dF/F time courses show lack of both CO_2 and diacetyl responses when Ab1B is selectively ablated (Cii, n=4 experimental, red, and n=3 control, black). Maximum response peaks are quantified for both odors (Ciii). **d,** CO_2 responses in VA2 are not from orco-negative terminals invading VA2. GCamP6f is expressed under the control of Pb-gal4, and dtx is expressed under the control of orco-lexA. VA2 responses are recorded using 2-photon imaging (Di). Average time courses show lack of responses in VA2 (Dii, n=3 experimental, red, and n=3 control, black). Maximum peaks are quantified as in C (Diii). The series of experiments shows CO_2 responses in VA2 reside in Ab1B terminals and do not represent responses from alien axons invading VA2. Odor stimuli were 10% CO_2, 10^{-5} diacetyl. Envelopes in average time courses, and error bars are SEMs.

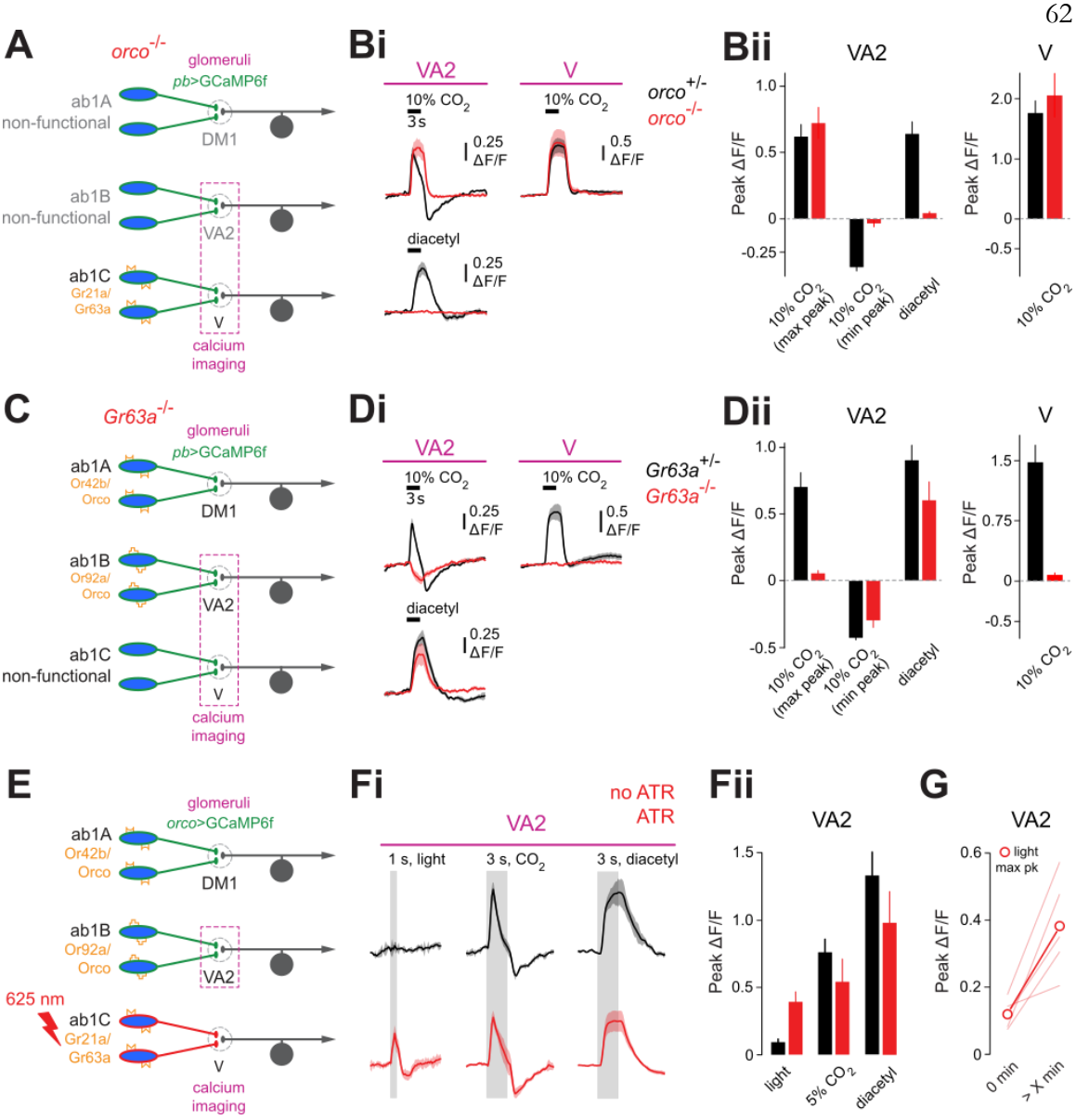

Figure 4: The inhibitory component of the CO_2 response is orco dependent, the excitatory component is Gr21a/Gr21a dependent. a, Schematic showing experimental setup**.** 2-photon calcium responses are recorded from VA2 and V in the orco mutant. GCaMP6f is expressed under the control of Pb-gal4. Mutating orco effectively silences all orco positive ORNs, including Ab1B. **b,** Average dF/F time courses in VA2 and V show excitatory CO_2 responses in VA2 persist even when the Ab1B cell bodies are silenced (Bi) (red: mutant, black: het control). Response peaks are quantified for VA2 and V (Bii). Odor stimuli are 10% CO_2 and 10^{-7} diacetyl (n=5 mutant, n=4 het control) **c,** Schematic of the

experimental setup. Responses are recorded from VA2 and V in the Gr63a mutant. **d**, Average time courses in VA2 and V show loss of excitatory CO_2 responses (Di) (red: mutant, black: het control). Note the persistence of inhibitory responses. Odor stimuli same as above**.** Quantification of peak amplitudes in VA2 and V (Dii) (n=5 mutant, n=4 het control). **e,** Schematic of the experimental setup. VA2 responses are recorded while optogenetically activating Ab1C. GCaMP is expressed under the control of Or83b-lexA, CsChrimson is expressed under the control of Gr21a-gal4. **f,** Average time courses show light induced responses in VA2 (Fi) (red: flies grown on ATR, black: flies grown without ATR), peaks of the responses are quantified (Fii). Stimuli are light, 5% CO_2, and 10^{-7} diacetyl (n=4-5 experimental, n=3 no ATR control). **g,** Switching of light induced responses from a low to high state. Plotted are maximum peak amplitudes of VA2 light responses in individual experiments, at the beginning and end of the experiment (red average, n=5).

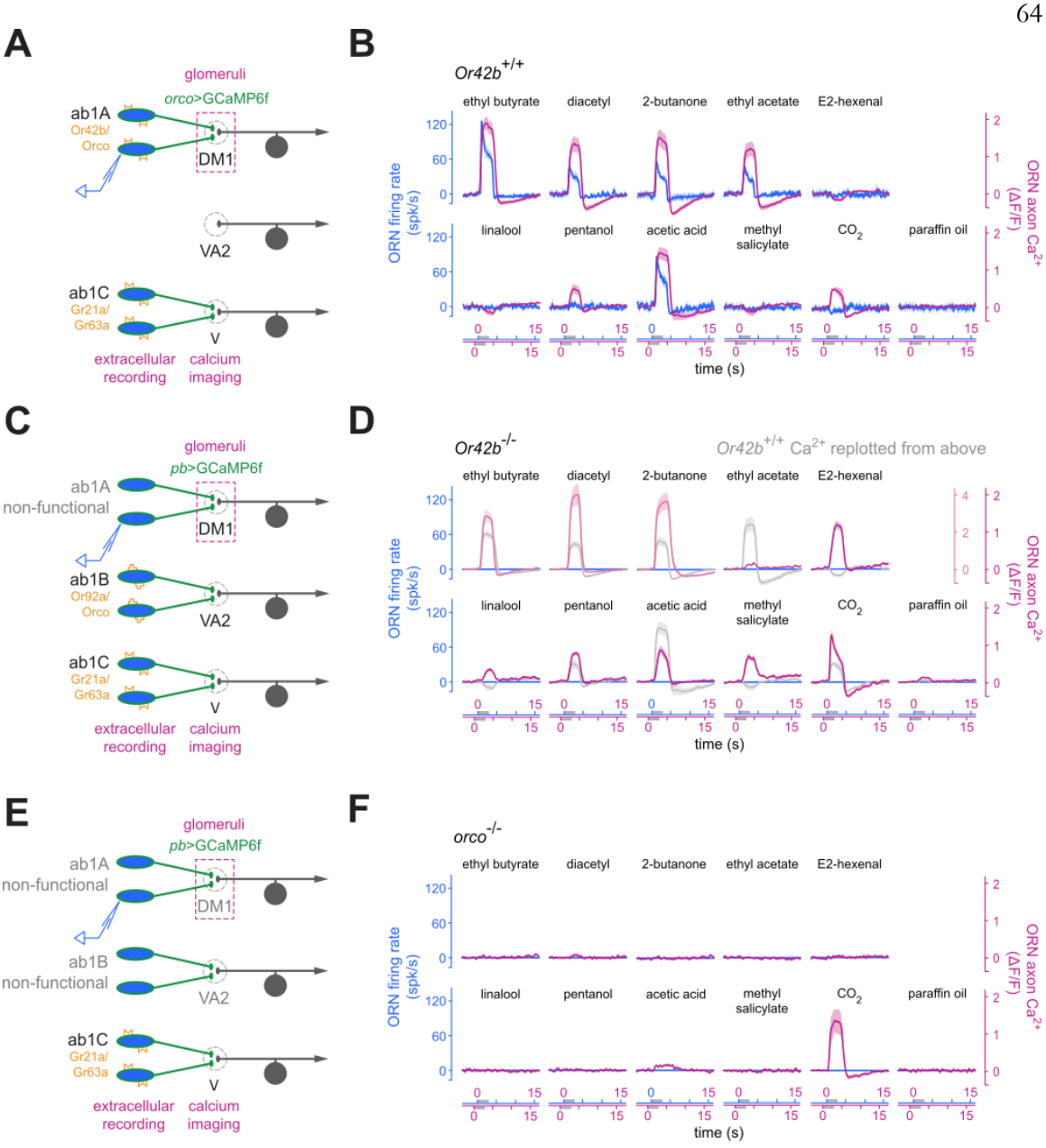

Figure 5: Mismatch in odor tuning between cell bodies and axon terminals of a different olfactory channel. a, Schematic showing the experimental setup. SSRs and calcium imaging experiments were conducted on Ab1A and DM1, respectively. Dtx was expressed under the control of Or92a-gal4, GCaMP6f was expressed under the control of Orco-lexA. This manipulation ablates Ab1B ORNs, allowing unambiguous identification of Ab1A spikes. **b,** PSTHs of Ab1A cell body responses are plotted (blue) (n=3) overlaid

on average dF/F time courses of the corresponding axons in DM1 (purple) (n=4-11). Note the absence of cell body responses to pentanol and CO_2. **c,** Schematic showing the experimental setup. SSRs and calcium imaging done in Ab1A and DM1, respectively with GCaMP6f being driven by Pb-Gal4 in the Or42b mutant background. The Or42b receptor mutation silences Ab1A cell body responses to odors. **d,** Sensillum PSTHs are plotted on top of average dF/F time courses from DM1 as before. Note the complete absence of responses in the cell body, and the residual responses in the axon terminals (n=3 electrophysiology, n=6-13 imaging). Calcium imaging responses from B are overlaid in gray for comparison. **e,** Schematic of the experimental setup. SSRs and calcium imaging in Ab1A and DM1, with GCaMP6f expressed under control of Pb-Gal4 in the Orco mutant background. **f,** Overlaid sensillum and terminal responses as in B,D. Note the collapse of all odor responses in both cell body and terminals with the exception of CO_2 responses in the axon terminals (n=3 electrophysiology, n=3-5 imaging).

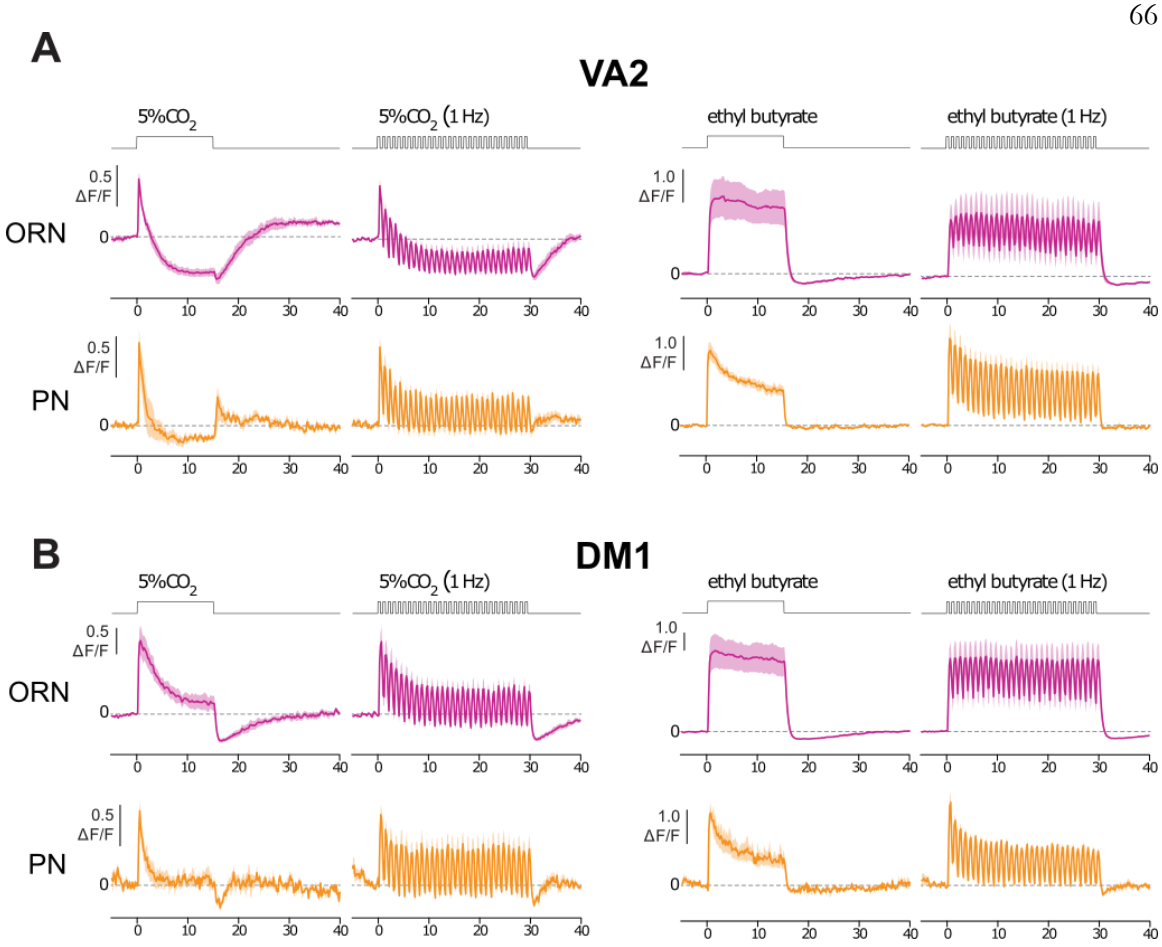

Figure 6: Interaction of inhibitory and excitatory components of CO_2 responses leads to selective filtering of CO_2 versus other odor stimuli. a, Average dF/F time courses in VA2 ORN terminals (purple, top row) in response to CO_2 presented as a 15s tonic stimulus or 30s pulsed stimulus pulsed at 1 Hz (left). These are in contrast to ORN terminal responses to ethyl butyrate also presented either tonically, or pulsed (right). Responses cross the ORN-PN synapse and are faithfully represented in the VA2 PN post-synaptic terminals (yellow, bottom row). Note that the pulsed CO_2 stimulus is faithfully propagated up to the PNs, while the tonic CO_2 stimulus is heavily filtered. In contrast, ethyl butyrate in the same glomerulus is faithfully represented up to the PNs when it is presented tonically, or pulsed. Inhibition interacts with excitation to selectively filter tonic CO_2 responses (n=4). **b,** Same as in A, but imaging done in DM1 ORN and PN terminals. DM1 shows the

same selective filtering. (n=4). All recordings done with GCaMP6f expressed under control of Pb-Gal4, odor stimuli were 5% CO_2, and 10^{-4} ethyl butyrate.

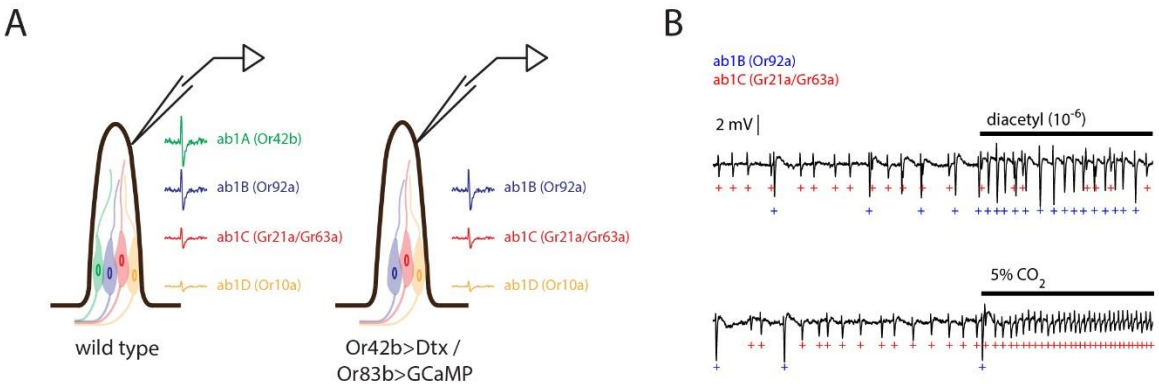

Extended Data Figure 1: CO_2 does not drive spiking responses at Ab1B cell bodies. a, Schematic of the recording setup. The wild-type Ab1 sensillum houses 4 ORNs: Ab1A, Ab1B, Ab1C, and Ab1D (left). Spikes elicited from Ab1C and Ab1D (red and orange), as measured via SSRs, have different amplitudes, and so can be easily told apart. However, Ab1A and Ab1B spikes (green and blue), have similar amplitudes, and are more difficult to sort. To unambiguously identify Ab1B spikes, we genetically ablated Ab1A ORNs via expression of a diphtheria toxin subunit (DTx) under the control of Or42b-gal4 (right) (GCaMP is also expressed in this line under the control of Or83b-gal4 for the imaging experiments in figure 3). With Ab1A ablated, Ab1B spikes can be easily differentiated from Ab1C and Ab1D activity. **b,** Voltage traces taken from a representative SSR in the Ab1A ablated line, showing Ab1B spikes in response to 10^{-7} diacetyl (top), and Ab1C spikes in response to 5% CO_2 (bottom). Note that there are no Ab1B spikes during CO_2 stimulation.

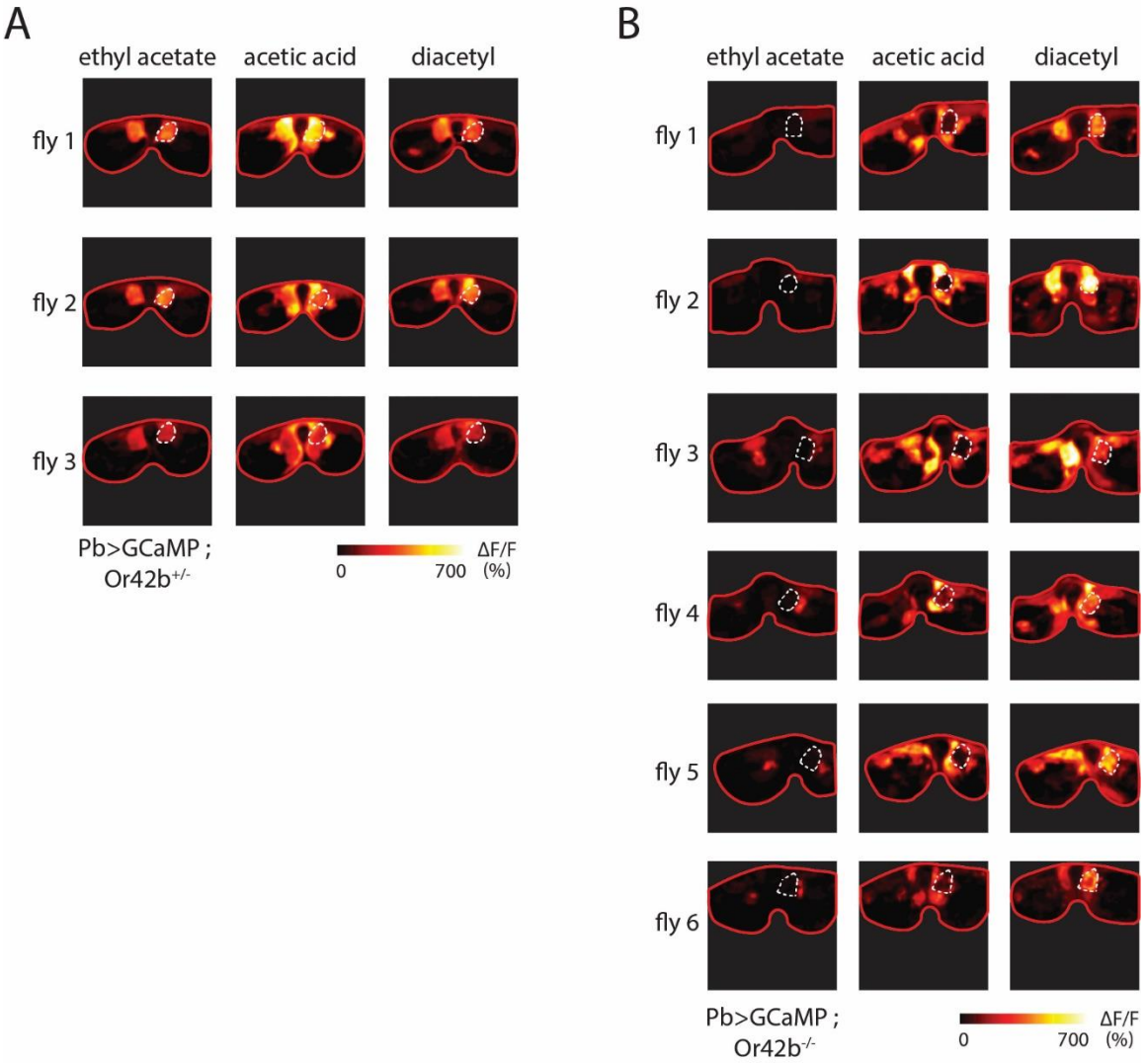

Extended Data Figure 2: Odor responses persist in Ab1A terminals when Ab1A cell bodies are silenced. a, Representative heat maps in response to 10^{-8} ethyl acetate, 1.5% acetic acid, and 10^{-4} diacetyl, in Pb-gal4,uas-opGCaMP6f;Or42[2]/SM6. Ethyl Acetate very specifically activates the DM1 glomerulus. Acetic acid and Diacetyl also drive DM1 responses. **b,** Representative heat maps as above, in Pb-gal4,uas-opGCaMP6f;Or42b[2] flies. Note the complete lack of ethyl acetate responses in DM1, and markedly reduced acetic acid responses. In contrast, note the persistence of diacetyl responses. Activation of additional glomeruli in response to ethyl acetate and diacetyl in the homozygous knock-

out as compared to the heterozygous control can be attributed to loss of inter-glomerular inhibition arising from DM1.

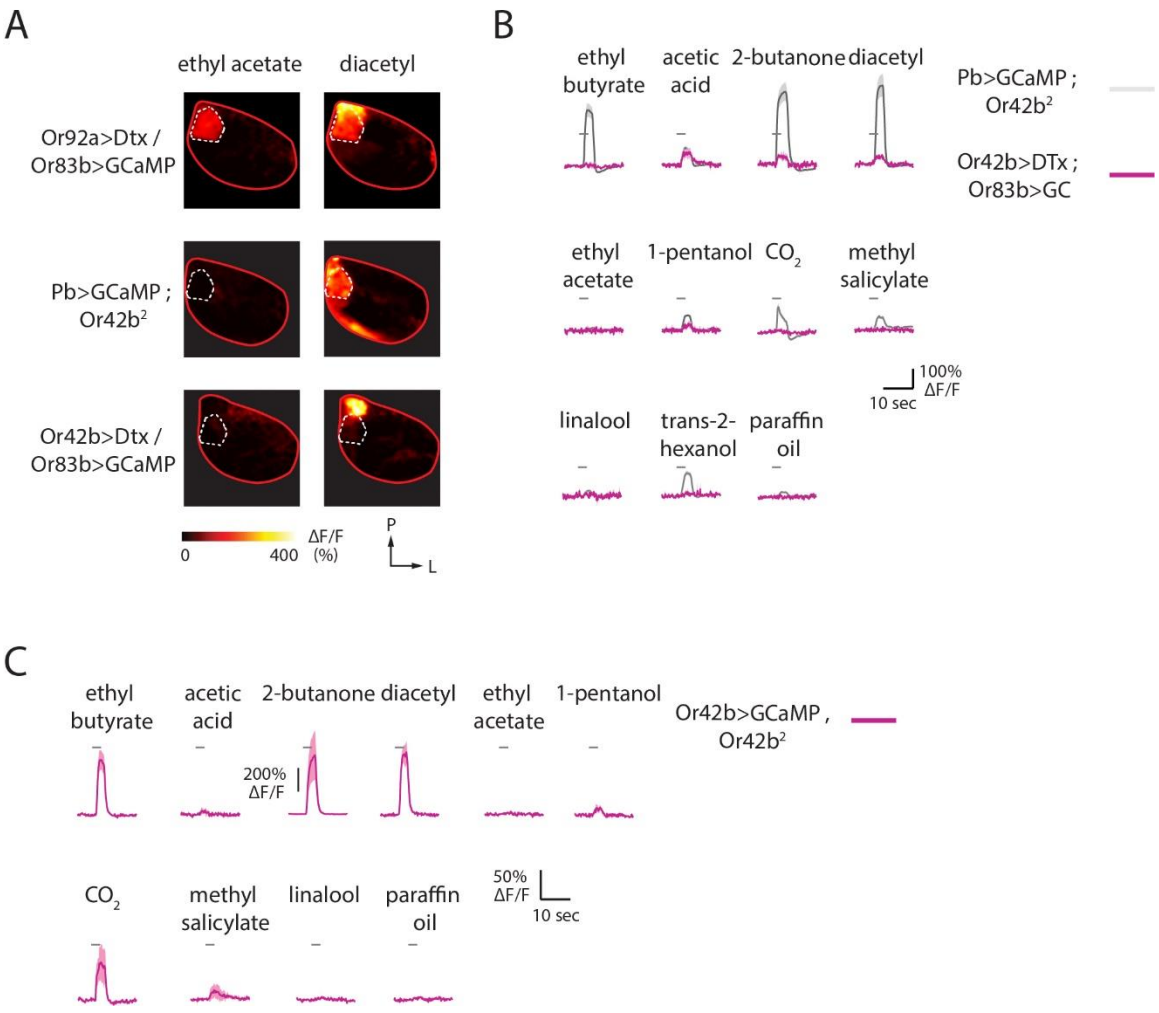

Extended Data Figure 3: Residual odor responses in Ab1A axon terminals when the Ab1A receptor is silenced are correctly identified as DM1 responses, and not due to out of plane fluorescence. a, Representative heat maps from the indicated genotypes, in response to 10^{-8} ethyl acetate, and 10^{-4} diacetyl. DM1 is outlined in blue. Flies with the Or42b receptor intact show responses to both ethyl acetate and diacetyl, in DM1 axon terminals (top row) (Ab1B ORNs have been genetically ablated in this line to facilitate identification of Ab1A spikes for the SSRs of figure 5). Flies with the Or42b receptor genetically silenced, lose DM1 responses to ethyl acetate, but retain responses to diacetyl (middle row). To determine whether the diacetyl responses are occurring in Ab1A axons, we then genetically ablate Ab1A using DTx. Flies with Ab1A ablated lose responses to

both ethyl acetate and diacetyl in DM1 (bottom row). The activation above the border of DM1 in response to diacetyl is a separate glomerulus, also visible in the top row diacetyl stimulation. **b,** Average dF/F time courses of responses in DM1 to the full odor panel of figure 5 with Ab1A ablated (pink) (n=3-4), overlaid on the responses when Or42b is silenced (light grey, data reused from Fig.5b). **c,** Average dF/F time courses of responses in DM1 to the full odor panel of figure 5, with Or42b mutated, and with GCaMP expressed under the control of Or42b-Gal4 (n=3). In this line, only DM1 is labelled with GCaMP, so that DM1 is unambiguously identified, and there is no out of plane signal from other glomeruli. Or42b is mutated, so that the Ab1A cell body is functionally silenced. DM1 (Ab1A axons) still responds to multiple odors in the tuning panel, confirming that the residual responses we measured in figure 5 are in fact arising from activity in Ab1A ORN axons.

from Fig.5b) *right*. The residual responses in the Or42b silenced line are not coming from out of plane fluorescence.

REFERENCES

1. Benton, R., Vannice, K.S., Gomez-Diaz, C., Vosshall, L.B. Variant ionotropic glutamate receptors as chemosensory receptors in *Drosophila*. *Cell* **136**, 149-62 (2009).
2. Hallem, E.A., Ho, M.G., Carlson, J.R., The molecular basis of odor coding in the *Drosophila* antenna. *Cell* **117**, 965–79 (2004).
3. Vosshall, L.B., Wong, A.M., Axel, R. An olfactory sensory map in the fly brain. *Cell* **102**, 147–59 (2000).
4. Hallem, E.A., Carlson, J.R., Coding of odors by a receptor repertoire. *Cell* **125**, 143-60 (2006).

5. Shang, Y., Claridge-Chang, A., Sjulson, L.,Pypaert, M., Miesenböck, G. Excitatory local circuits and their implications for olfactory processing in the fly antennal lobe. *Cell* **128**, 601–12 (2007).
6. Olsen, S.R., Bhandawat, V., Wilson, R.I. Excitatory interactions between olfactory processing channels in the *Drosophila* antennal lobe. *Neuron* ***54,*** 89–103 (2007).
7. Root, C.M., Semmelhack, J.L., Wong, A.M., Flores, J., Wang, J.W., Propagation of olfactory information in *Drosophila*. *PNAS* 104,11826–31 (2007).
8. Bhandawat, V., Olsen, S.R., Schlief, M.L., Gouwens, N.W., Wilson, R.I. Sensory processing in the *Drosophila* antennal lobe increases the reliability and separability of ensemble odor representations. *Nat Neurosci* **10**, 1474–82 (2007).
9. Olsen, S.R., Wilson, R.I. Lateral presynaptic inhibition mediates gain control in an olfactory circuit. *Nature* **452**, 956–60 (2008).
10. Root, C.M., Masuyama, K., Green, D.S, Enell, L.E.,Nassel, D.R., et al.A presynaptic gain control mechanism fine-tunes olfactory behavior. *Neuron* ***59,*** 311–21 (2008).
11. Yaksi, E., Wilson, R.I. Electrical coupling between olfactory glomeruli. *Neuron*. **67**, 1034–47 (2010).
12. Huang, J., Zhang, W., Qiao, W., Hu, A., Wang, Z. Functional connectivity and selective odor responses of excitatory local interneurons in *Drosophila* antennal lobe. *Neuron* 67,1021–33 (2010).
13. Jones, W.D., Cayirlioglu, P.,Kadow, I.G., Vosshall, L.B. Two chemosensory receptors together mediate carbon dioxide detection in *Drosophila*. *Nature* **445**, 86-90 (2007).
14. Kwon, J.Y., Dahanukar, A., Weiss, L.A., Carlson, J.R. The molecular basis of CO2 reception in *Drosophila*. *Proc. Natl. Acad. Sci. USA* **104**, 3574-3578 (2007).
15. Suh, G.S., Wong, A.M., Hergarden, A.C., Wang, J.W., Simon, A.F., Benzer, S., Axel, R., Anderson, D.J. A single population of olfactory sensory neurons mediates an innate avoidance behaviour in *Drosophila*. *Nature* **431**, 854-859 (2004).

16. De Bruyne, M., Foster, K.,Carlson, J.R. Odor coding in the *Drosophila* antenna. *Neuron* **30** 537–52 (2001).
17. Larsson, M. et al. *Or83b* encodes a broadly expressed odorant receptor essential for Drosophila olfaction. *Neuron* **43**, 703–714 (2004).
18. Kazama, H., Wilson, R.I. Homeostatic matching and nonlinear amplification at genetically-identified central synapses. *Neuron* **58**, 401–13 (2008).
19. Olsen, S.R., Bhandawat, V., Wilson, R.I. Divisive normalization in olfactory population codes. *Neuron* **66**, 287–99 (2010).
20. Asteriti, S., Gargini, C., Cangiano, L. Mouse rods signal through gap junctions with cones. *Elife Sci.* 3, 162–171 (2014).
21. Raviola, E., Gilula, N.B. Gap junctions between photoreceptor cells in the vertebrate retina. *Proc Natl Acad Sci USA* . 70, 1677–1681 (1973).
22. Rabinowitch, I., Chatzigeorgiou, M., Schafer, W.R. A gap junction circuit enhances processing of coincident mechanosensory inputs. *Curr. Biol*. **23**, 963–967 (2013).
23. Root, C.M., Ko, K.I., Jafari, A., Wang, J.W. Presynaptic facilitation by neuropeptide signaling mediates odor-driven food search. *Cell* **145**, 133–44 (2011).
24. Van Breugel, F., Huda, A., Dickinson, M.H. Distinct activity-gated pathways mediate attraction and aversion to CO2 in Drosophila. *Nature*. **564**, 420–424 (2018).
25. Wasserman, S., Salomon, A. & Frye, M.A. *Drosophila* tracks carbon dioxide in flight. *Curr. Biol*. **23**, 301–306 (2013).
26. Suh, G.S.B., et al. Light activation of an innate olfactory avoidance response in Drosophila. *Curr. Biol.* **17**, 905–908 (2007).
27. Bell, J.S., Wilson, R.I.Behavior reveals selective summation and max pooling among olfactory processing channels. *Neuron* **91**, 425–438 (2016).
28. Semmelhack, J.L., Wang, J.W. Select *Drosophila* glomeruli mediate innate olfactory attraction and aversion. *Nature* **459**, 218–223 (2009)